

0 280  
50280/1133  
**ACTA UNIVERSITATIS SZEGEDIENSIS**

---

# **ACTA PHYSICA ET CHEMICA**

**NOVA SERIES**

**TOMUS XXXIV**

**FASCICULI 1—4.**

**AUSHAF 34 (1—4) 1988**

**HU ISSN 0324—6523 Acta Univ. Szeged**

**HU ISSN 0001—6721 Acta Phys. et Chem.**

**SZEGED, HUNGARIA**

**1988**

---

ACTA UNIVERSITATIS SZEGEDIENSIS

---

# ACTA PHYSICA ET CHEMICA

NOVA SERIES

TOMUS XXXIV

FASCICULI 1—4.

AUSHAF 34 (1—4) 1988

HU ISSN 0324—6523 Acta Univ. Szeged

HU ISSN 0001—6721 Acta Phys. et Chem.

SZEGED, HUNGARIA

1988

---

Adiuvantibus

M. BARTÓK, K. BURGER, L. CSÁNYI, J. CSÁSZÁR, P. FEJES, I. HEVESI, P. HUHN,  
I. NAGYPÁL, E. KAPUY, I. KETSKEMÉTY, F. SOLYMOSI, et F. SZÁNTÓ

Redigit  
MIKLÓS I. BÁN

Edit  
Facultas Scientiarum Universitatis Szegediensis de  
Attila József nominata

Editionem curant  
J. ANDOR, I. BÁRDI, Á. MOLNÁR, et Á. SÜLI

Nota  
Acta Phys. et Chem. Szeged

---

Szerkeszti  
BÁN MIKLÓS

A szerkesztőbizottság tagjai:  
BARTÓK M., BURGER K., CSÁNYI L., CSÁSZÁR J., FEJES P., HEVESI I.,  
HUHN P., NAGYPÁL I., KAPUY E., KETSKEMÉTY I., SOLYMOSI F., és SZÁNTÓ F.

Kiadja:  
a József Attila Tudományegyetem Természettudományi Kara  
(Szeged, Aradi vértanúk tere 1.)

Szerkesztőbizottsági titkárok:  
ANDOR J., BÁRDI I., MOLNÁR Á., és SÜLI Á.

Kiadványunk rövidítése:  
Acta Phys et. Chem. Szeged

ON THE ERROR OF THE ABSORPTION COEFFICIENTS  
OF WEAKLY ABSORBING THIN LAYERS, DETERMINED  
FROM TRANSMITTANCE MEASUREMENTS

By

L. MICHAILOVITS, M.I. TÖRÖK AND I. HEVESI

Institute of Experimental Physics, József Attila University,  
Szeged, Dóm tér 9., HUNGARY

(Received 20 June, 1988)

The absorption coefficient,  $k(\lambda)$ , calculated from the transmittance is very sensitive to the errors in thickness and refractive index. The error in  $k(\lambda)$  is relatively small at the wavelengths of the extrema of transmittance but more pronounced between them, yielding a characteristic wobbling in the absorbance spectrum calculated.

The fringe pattern of the measured transmittance spectrum can be used to determine the optical constants (refractive index  $n(\lambda)$  and absorption coefficient  $k(\lambda)$ ) of semiconductor or insulator layers. We earlier proposed an improved [1] method for the determination of the optical constants and thickness of weakly absorbing ( $n \gg k$ ) films deposited on thick transparent substrates [2, 3]. In a recent paper [4], we showed that the coefficient of absorbance,  $k$  can be determined with high accuracy in a wide range of wavelengths when the index of refraction,  $n = n(\lambda)$  satisfies the disper-

sion relation of the classical oscillator model [5].

In the present work, we discuss the influences of the error in measured transmittance,  $n(\lambda)$  and  $d$  on the  $k(\lambda)$  spectrum determined using the method outlined in [4]. Instead of making complicated and not very impressive error calculations we will call attention to the effects of the mentioned errors by presenting simple numerical results obtained by analysis of simulated transmittance spectra.

#### The method

In the usual thin-film geometry a weakly absorbing layer ( $n \gg k$ ) deposited onto a thick transparent substrate ( $d_s \gg \lambda$ ) should be considered (Fig. 1). The transmittance of

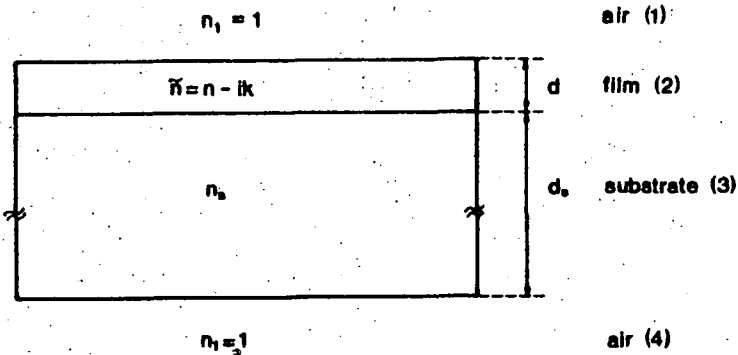


Figure 1.: Typical sample structure for transmittance measurement on a thin film. The refractive index is denoted by  $n$ , the absorption coefficient is  $k$  and the thickness of the film is  $d$ .

a thin, weakly absorbing film on a non-absorbing substrate is described in [6] as follows:

$$T = \frac{T_{31} T_{34}}{1 - R_{31} R_{34}}, \quad (1)$$

where  $T_{31}$  denotes the transmittance of the light travelling from the air through the film into the substrate, and  $R_{31}$  is the reflectance of the same surface.  $T_{34}$  and  $R_{34}$  relate to the substrate/air interface. These quantities can be calculated as follows:

$$T_{31} = \frac{n_s^2 \tau_{12}^2 \tau_{23}^2}{\exp(\delta) + \rho_{12}^2 \rho_{23}^2 \exp(-\delta) - 2\rho_{12} \rho_{23} \cos(\varphi_{12} + \varphi_{23} + \alpha)} \quad (2)$$

$$R_{31} = \frac{\rho_{12}^2 \exp(\delta) + \rho_{23}^2 \exp(-\delta) - 2\rho_{12} \rho_{23} \cos(\varphi_{23} - \varphi_{12} + \alpha)}{\exp(\delta) + \rho_{12}^2 \rho_{23}^2 \exp(-\delta) - 2\rho_{12} \rho_{23} \cos(\varphi_{12} + \varphi_{23} + \alpha)} \quad (3)$$

$$T_{34} = \frac{4n_s}{(n_s + 1)^2}, \quad (4)$$

$$R_{34} = \left( \frac{n_s - 1}{n_s + 1} \right)^2. \quad (5)$$

The quantities in (2) and (3) are expressed by the optical constants of the layer,  $n$  and  $k$ , and the refractive index of the substrate,  $n_s$ , as follows:

$$\tau_{12}^2 = \frac{4}{(n+1)^2 + k^2}, \quad (6)$$

$$\tau_{23}^2 = \frac{4(n^2+k^2)}{(n_s+n)^2+k^2}, \quad (7)$$

$$\rho_{12}^2 = \frac{(n-1)^2+k^2}{(n+1)^2+k^2} \quad (8)$$

$$\rho_{23}^2 = \frac{(n_s-n)^2+k^2}{(n_s+n)^2+k^2}, \quad (9)$$

$$\operatorname{tg} \varphi_{12} = \frac{2k}{n^2+k^2-1}, \quad (10)$$

$$\operatorname{tg} \varphi_{23} = \frac{2kn_s}{n^2+k^2-n_s^2}, \quad (11)$$

$$\alpha = \frac{4\pi nd}{\lambda}, \quad (12)$$

$$\delta = \frac{4\pi kd}{\lambda}. \quad (13)$$

For the range of wavelengths, if the layer is weakly absorbing ( $n \gg k$ ), Eq. (1) can be simplified and the extrema of the transmittance  $T(\lambda)$  can be expressed as

$$T_{\text{extr.}} = \frac{16n^2 n_s \eta}{(n+1)^3 (n_s^2+n)^2 - (n-1)^3 (n_s^2-n)^2 + (-1)^m 2(n^2-1)(n_s^2-n^2)\eta}, \quad (14)$$

where

$$\eta = \exp\left(-\frac{4\pi kd}{\lambda}\right), \quad (15)$$

and  $m$  denotes the order of interference satisfying the rela-

tion

$$\frac{4\pi}{\lambda}nd = m\pi, \quad (16)$$

or, to a good approximation

$$m = \frac{\lambda_{m+1}}{\lambda_m - \lambda_{m+1}}. \quad (17)$$

Here  $\lambda_m$  and  $\lambda_{m+1}$  denote the wavelengths of two neighbouring extrema.

From the measured transmittance of the system film-substrate, one can obtain the maximum and minimum values of the spectrum and the corresponding wavelengths. Using the relations (14-17) or the method presented in [2,3] at the wavelengths relating to the extrema, the optical constants and the thickness of the layer can be determined. If the refractive index of the substrate,  $n_g(\lambda)$ , is also unknown, it can be determined from one transmittance measurement before the deposition of the film.

If the calculated  $n(\lambda_m)$  values lie on a straight line in  $1/(n^2-1)$  vs  $1/\lambda^2$  plot (i.e. the function  $n = n(\lambda)$  behaves as predicted by the classical oscillator model [5]), then this line can be used to interpolate or extrapolate the refractive index at any wavelength. Now, Eqs (1)-(3) allow the determination of  $K(\lambda) = (4\pi/\lambda) \cdot k(\lambda)$  at any wavelength, from measured  $T(\lambda)$  and calculated  $n(\lambda)$  and  $d$  values [4].



*Analysis of possible errors by using  
simulated transmittance spectra*

As the first step we constructed a transmittance spectrum (Fig. 2) from given  $n(\lambda)$ ,  $k(\lambda)$ ,  $n_s(\lambda)$  functions and thickness  $d$  with help of Eqs (1)-(13). The  $n(\lambda)$  and  $n_s(\lambda)$  functions were chosen to fulfil the conditions of the clas-

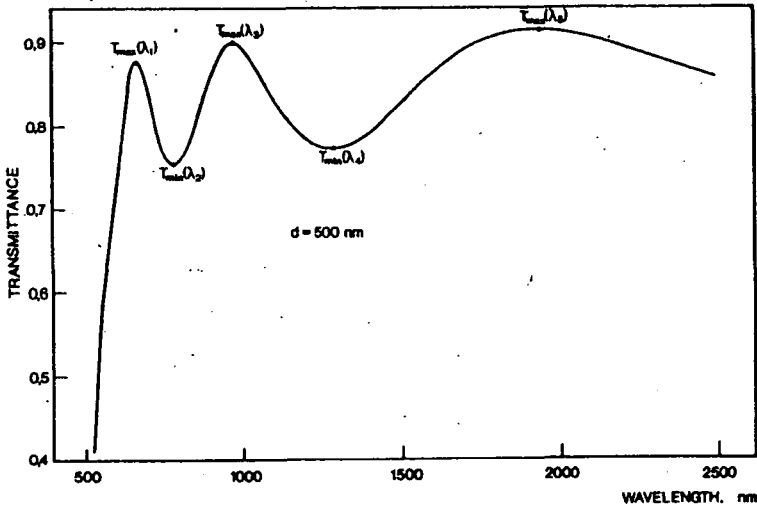


Figure 2.: Simulated transmittance spectrum with fringe pattern

sical oscillator model (Figs 3 and 4). The absorption coefficient is given as.

$$k(\lambda) = a \cdot \exp(-b \cdot \lambda) + c$$

(where  $a = 1.55 \cdot 10^6$ ;  $b = 3.26 \cdot 10^{-2}$ ;  $c = 4.5 \cdot 10^{-3}$ ). This original  $k(\lambda)$  function appears as the full curve in Figs 5-7. The thickness was chosen as 500 nm. From the  $T(\lambda)$  spectrum constructed in this way, the  $n$ ,  $k$  and  $d$  values were determined at the wavelengths  $\lambda_1, \lambda_2, \dots$  via the fringe pattern method described in [1,3]. The obtained  $n$  and  $k$  values are

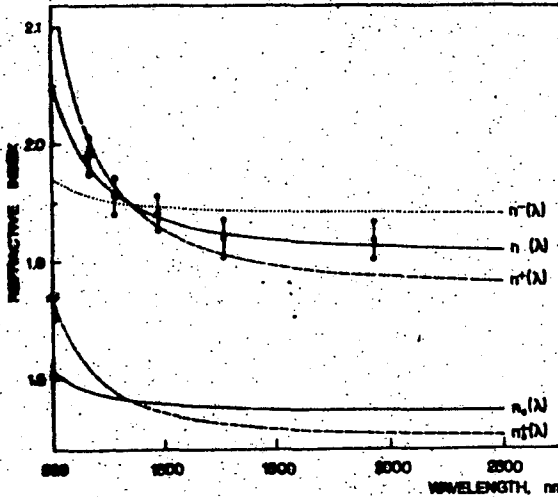


Figure 3.: Wavelength-dependence of the refractive indices  $n$  and  $n_g$ , constructed by means of the classical oscillator model.

shown as full circles in Figs 3-7. For comparison we calculated then,  $k$  and  $d$  values at the same wavelengths from the transmittance spectra

$$T^+(\lambda) = T(\lambda) + 0.003$$

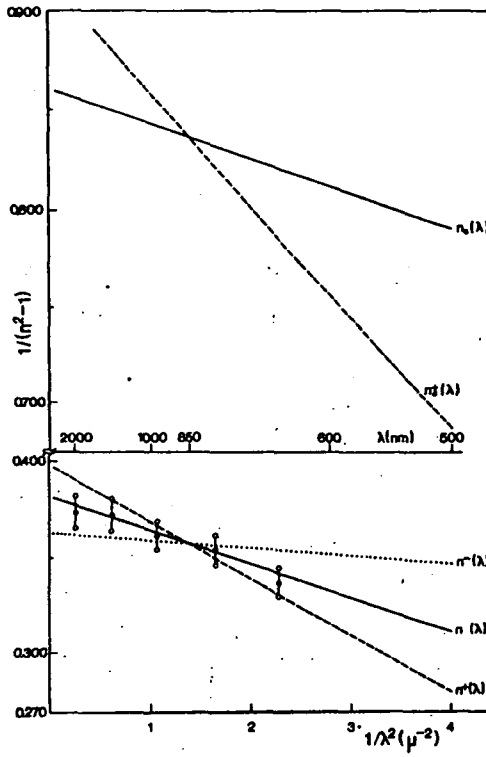


Figure 4.: The refractive indices  $n$  and  $n_s$  of Fig. 3, replotted as  $1/(n^2-1)$  vs.  $1/\lambda^2$ .

and

$$T^-(\lambda) = T(\lambda) - 0.003$$

too. The obtained values are given as empty circles in

Figs 3-7. The original and the calculated values of the optical constants and thicknesses are listed in Table I. When the data given in this Table are compared, it can be concluded that the error in the procedure is less than that caused by the uncertainty in the measurement.

We shall examine now the change in the  $k(\lambda)$  spectrum calculated from  $T(\lambda)$  when the values of  $n(\lambda)$ ,  $n_g(\lambda)$  and  $d$  differ from the originals. The deviations in  $n(\lambda)$  and  $n_g(\lambda)$

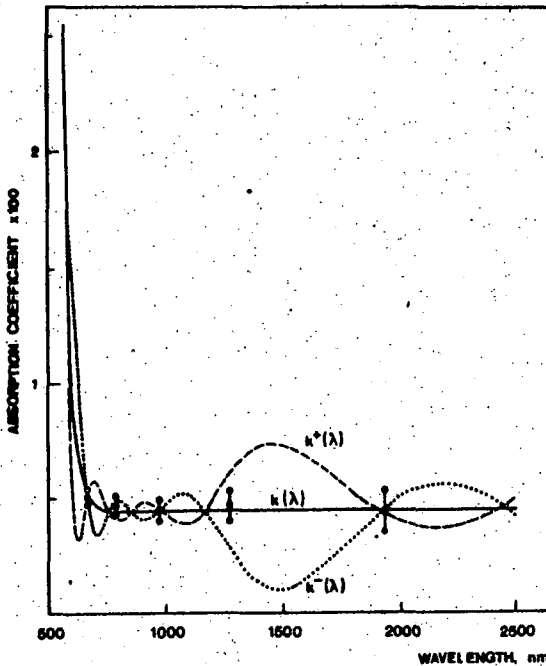


Figure 5.: Absorption spectra. Full line: original curve, constructed with the expression  $a \cdot \exp(-b \cdot \lambda) + c$ ; dotted and dashed lines: calculated from the transmittance, using  $n^+(\lambda)$  and  $n^-(\lambda)$ .

where chosen according to the following conditions: the difference between the original and new values is 2 per cent at  $\lambda = 600$  nm and zero at  $\lambda = 850$  nm; and the dispersion relation also holds for the new set of data. The new functions are denoted by  $n^+$ ,  $n^-$  and  $n_g$  in Figs 3 and 4. The new thicknesses are 490 and 510 nm, corresponding to a 2 per cent change.

The  $k(n, n_g, d, T)$  values were calculated by using the new set of data. The  $k^+(\lambda)$  and  $k^-(\lambda)$  curves (Fig. 5) were obtained by using the new  $n^+(\lambda)$  and  $n^-(\lambda)$  values, while the data in Figs 6 and 7 were calculated with new  $d$  values and

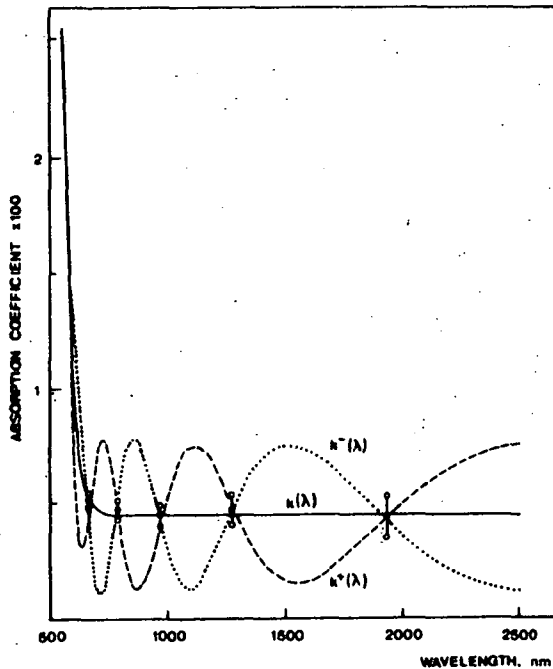


Figure 6.: Adsorption spectra. Full line: original; dotted and dashed lines: calculated, using  $d^+$  and  $d^-$ .

Table I

$\lambda_m$ (nm)	ORIGINAL			CALCULATED from T			CALCULATED using $T \pm \Delta T$		
	n	$k \cdot 10^3$	d	n	$k \cdot 10^3$	d	n	$k \cdot 10^3$	d (nm)
663	1.981	5.2	500 nm	1.991	5.1	499	1.974-2.006	4.0-5.4	504-496
780	1.958	4.5		1.956	4.9	498	1.940-1.972	4.7-5.5	503-494
970	1.938	4.5		1.941	4.5	500	1.926-1.956	4.0-4.9	504-496
1270	1.924	4.5		1.920	4.8	496	1.903-1.935	4.4-5.6	501-492
1935	1.913	4.5		1.918	4.5	504	1.902-1.933	3.5-5.3	509-501

$n_s(\lambda)$  function, respectively. All the other parameters were kept unaltered.

Comparison of  $k(\lambda)$  with  $k^+(\lambda)$  and  $k^-(\lambda)$  (Figs 5-7) reveals that in the range of weak absorption there is a considerable and characteristic deviation. From Figs 5-7, it is apparent that relatively small deviations from the original  $n(\lambda)$  and  $d$  values result in dramatic changes in the  $k(\lambda)$  spectra, while the uncertainty in  $n_s(\lambda)$  causes only minor

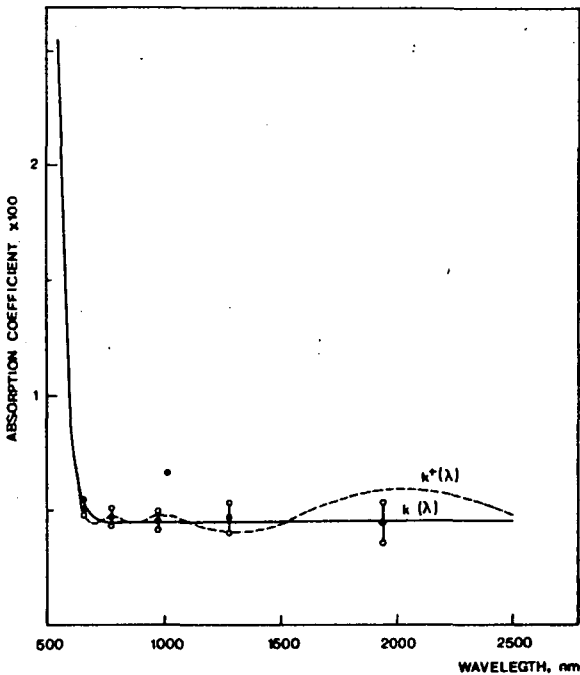


Figure 7.: Absorption spectra. Full line: original; dashed line: calculated using  $n_s$ .

differences. This effect is less pronounced in the range of strong absorption. The characteristic periodicity in the  $k^+(\lambda)$  and  $k^-(\lambda)$  spectra is due to the fact that, the insertion of inappropriate  $n(\lambda)$  and  $d$  values into the interference term of Eqs (2) and (3) results in large deviations in arc.

The results of the above model calculations confirm that the method described in [1] is well suitable for the determination of  $k(\lambda)$ , if the  $d$  and  $n(\lambda)$  data used are correct enough. Any fluctuation calls for a revision of the precision of the  $n$  and  $d$  values used. On the other hand, the difference between two adjacent minima and maxima of  $k(\lambda)$  can be regarded as the error of the absorption constant determined.

#### References

- [1] Valeev, A.C.: Opt. Spektrosk., 15, 269 (1963).
- [2] Michailovits, L., I. Hevesi, Liem Phan, Zs. Varga: Thin Solid Films, 102, 71 (1983).
- [3] Török, M.I.: Opt. Acta, 32, 479 (1985).
- [4] Michailovits, L., M. I. Török, I. Hevesi: Thin Solid Films, 139, 143 (1986).
- [5] Moss, T.S.: Optical Properties of Semiconductors, Butterworths, London, 1961, Chapter 2.
- [6] Born, M., E. Wolf: Principles of Optics, Pergamon, Oxford, 1964, Section 13.4.



О НЕТОЧНОСТИ КОЭФФИЦИЕНТА ПОГЛОЩЕНИЯ СЛАБО ПОГЛОЩАЮЩИХ ТОНКИХ ПЛЕНОК, ОПРЕДЕЛЕННОГО ПО ИЗМЕРЕНИИ СПЕКТРА ПРОПУСКАНИЯ

Л. Михайлович, М. И. Терек и И. Хевеши .

Коэффициенты поглощения  $\kappa(\lambda)$  рассчитанные по пропусканию очень чувствительны к неточностям определения толщины слоя и показателя преломления.

Ошибка в  $\kappa(\lambda)$  относительно мала при экстремальных значениях пропускания и более значительна между ними которое приводит к характерным неровностям в рассчитанном спектре.

COMPARISON OF UV SPECTRA OF AROMATIC SCHIFF BASES AND  
THEIR REDUCTION PRODUCTS; POSSIBILITY OF ASSIGNMENT  
OF  $\pi^* + n$  TRANSITION OF AZOMETHINE GROUP

By

J. CSÁSZÁR

Institute of General and Physical Chemistry, József Attila University,  
H-6701, Szeged, P.O.B. 105, Hungary

*(Received 9 August 1988)*

The UV spectra of Schiff bases of 4-X-N(2-hydroxybenzylidene)aniline type ( $X = C_2H_5, OC_2H_5, CH_3, OCH_3, H, Cl, Br$ ) and their reduction products obtained via  $NaBH_4$  reduction were studied, primarily with regard to the appearance of the  $\pi^* + n$  transition characteristic of the azomethine group.

The spectra of Schiff bases prepared from salicylaldehyde with aliphatic mono- and diamines [1], aniline [2-5] and pyridine [6] derivatives, and their molecular conformations [7] were discussed previously, the absorption spectra of the secondary amines obtained from the above Schiff bases via  $NaBH_4$  reduction have also been described [8].

The present paper compares the spectra of the Schiff bases (I) and those of their reduction products (II), containing  $-CH=N-$  and  $-CH_2-NH-$  linkages, respectively, and dis-



Table I

Spectral data of several Schiff bases and the corresponding secondary amine

X	Typ	Solv*	$\lambda/nm$ and $\log \epsilon$				
C <sub>2</sub> H <sub>5</sub>	SB	Hex.	211 (4.28)	232 (4.33)	269 (4.11)	344 (4.13)	430 (2.48)
		MeOH		228 (4.28)	270 (4.03)	342 (4.10)	
	SA	Hex.	210 (4.39)	238 (4.37)	278 (3.78)	~295	
MeOH		203 (4.86)	246 (4.36)	~280	~310		
OC <sub>2</sub> H <sub>5</sub>	SB	Hex.	212 (4.24)	233 (4.28)	269 (4.01)	350 (4.22)	430 (2.46)
		MeOH		230 (4.22)	268 (3.96)	346 (4.21)	
	SA	Hex.	207 (4.32)	236 (4.19)	279 (3.56)	~300	
MeOH		203 (4.58)	243 (4.18)	~275	310 (3.43)		
CH <sub>3</sub>	SB	Hex.	210 (4.30)	231 (4.35)	269 (4.12)	346 (4.16)	430 (2.40)
		MeOH		228 (4.32)	269 (4.02)	340 (4.10)	
	SA	Hex.	209 (4.39)	235 (4.35)	279 (3.71)	~295	
MeOH		203 (4.67)	244 (4.14)	~277	~300		
OCH <sub>3</sub>	SB	Hex.	212 (4.36)	230 (4.37)	269 (4.10)	350 (4.28)	430 (2.43)
		MeOH		224 (4.19)	274 (3.95)	347 (4.18)	
	SA	Hex.	207 (4.26)	234 (4.13)	279 (3.47)	~305	
MeOH		203 (4.28)	241 (4.15)	~275	304 (3.22)		
H	SB	Hex.	209 (4.37)	229 (4.42)	268 (4.23)	344 (4.15)	435 (2.26)
		MeOH		224 (4.27)	269 (3.98)	340 (3.93)	
	SA	Hex.	208 (4.23)	233 (4.18)	279 (3.60)	?	
MeOH		205 (4.50)	246 (4.16)	276 (3.53)	~310		
Cl	SB	Hex.	213 (4.43)	233 (4.47)	272 (4.31)	347 (4.27)	436 (4.04)
		MeOH		230 (4.34)	272 (4.16)	342 (4.14)	
	SA	Hex.	207 (4.32)	243 (4.31)	278 (3.60)	~300	
MeOH		206 (4.19)	255 (3.98)	~280	307 (4.21)		
Br	SB	Hex.	212 (4.33)	232 (4.39)	270 (4.24)	344 (4.21)	434 (2.02)
		MeOH		228 (4.42)	274 (4.07)	344 (4.10)	
	SA	Hex.	208 (4.41)	244 (4.32)	278 (3.67)	~305	
MeOH		205 (4.56)	256 (4.35)	~280	307 (3.23)		

\* SB: Schiff base, SA: secondary amine,  
Hex: n-hexane, MeOH: methanol

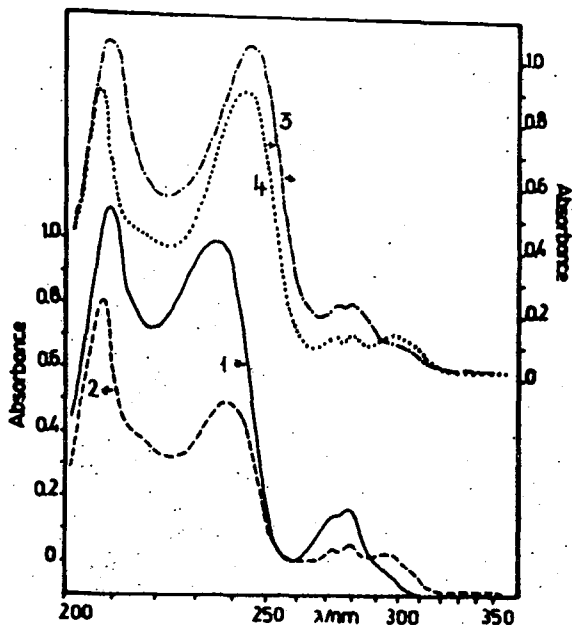
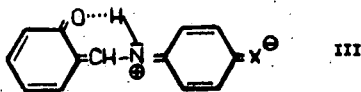


Figure 1.: UV spectra of 1: salicylidene-p-toluidine;  
 2: o-cresol + p-toluidine;  
 3: salicylidene-p-Cl-aniline;  
 4: o-cresol + p-Cl-aniline.  $c = 5 \cdot 10^{-4} \text{ mol/dm}^3$ ,  
 $d = 0.1 \text{ cm}$ .

The three bands mentioned correspond to perturbed benzene bands ( $E_{1u}$ ,  $B_{1u}$ ,  $B_{2u} + A_{1g}$ ). This assignment is supported by the high intensities of the bands, the splitting of the long-wavelength band, and the fact that the  $\lambda_3/\lambda_2$  values lie in the interval 1.15-1.20, which differs only slightly from that obtained for the monosubstituted benzene derivatives [13]. The bands shift bathochromically on going from n-hexane to methanol. Of course, a detailed assignment is difficult, because the  $\pi^* + \pi$  bands of the aldehyde and

aniline parts overlap.

The spectra of the Schiff bases are more complicated, since these three chromophores and their interactions must be taken into account. The spectra of the Schiff bases differ markedly from those of the corresponding secondary amines (Fig. 2). The difference is understandable for, with the transmission of the azomethine group, a uniform conjugated system involving the whole molecule is present (III)



and the lone-pair of the nitrogen atom also takes part in the conjugation, to an extent depending on the dihedral angle [7].

Since the Schiff bases and the secondary amines studied differ only in the connecting bridge between the two aromatic systems, a comparison of their spectra is important. Characteristic features in the spectra are the high-intensity bands of the  $\pi^* + \pi$  transitions. The band due to the  $\pi^* + n$  transition of the non-bonding lone-pair electrons of the azomethine group is not readily observable, because this is relatively weak in intensity as compared to the  $\pi^* + \pi$  type transitions. The  $\pi^* + n$  transitions within the aromatic nucleus are also important, but this problem will not be dealt with now.

The unconjugated azomethine group gives a weak band in the range 230-250 nm, with  $\log \epsilon \sim 1.8-2.5$  [14, 15]. The band disappears on acidification of the solution, supporting the postulate that the lone-pair electrons are involved in the transition [15, 16]. Platt [17] and Sindman [18] estimated that the  $\pi^* + n$  transition lies at  $\sim 210$  nm if the azomethine

group carries aliphatic substituents, and at ~250 nm or at ~290 nm if it is conjugated with a vinyl group or with a benzene ring. Because of the difficulty of assignment, the interpretation of the long-wavelength absorption of the Schiff bases and the assignment of the  $\pi^* \leftarrow n$  transition have been the subjects of several conflicting reports [e.g. 24].

We have prepared several Schiff bases containing an n-butyl group on the carbon or on the nitrogen and of the azomethine group. The spectrum of butylidene-n-butylamine (Fig. 2) exhibits only a single band (236 nm,  $\log \epsilon = 2.30$ ),

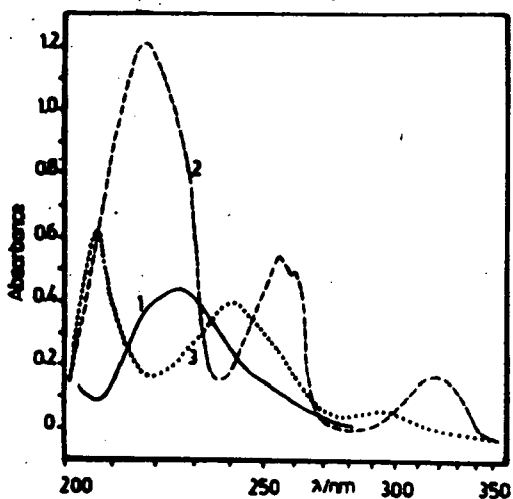


Figure 2.: UV spectra of 1: butylidene-n-butylamine; 2: salicylidene-n-butylamine; 3: n-butylidene-p-toluidine.  $c=5 \cdot 10^{-4}$  mol/dm<sup>3</sup>,  $d=1.0$  (1), 0.1 cm (2,3)

which can be assigned, in all likelihood, to the  $\pi^* + n$  transition. The maximum moves to higher frequencies on change from non-polar to hydroxylic solvents with high permittivity, which is characteristic of the  $\pi^* + n$  transition [19-21]. The spectra of benzylidene-n-butylamine (246 and 280 nm,  $\log \epsilon = 4.16$  and 3.13) and butylidene-aniline (235 and 287 nm,  $\log \epsilon = 4.03$  and 3.42) differ only slightly from those of benzaldehyde and aniline, respectively, but the curves are flattened towards longer wavelengths, showing the presence of a low-intensity band, which may be located at around 300 and 320 nm, respectively. This band is presumably a  $\pi^* + n$  band which, as a consequence of the conjugation, displays a bathochromic shift. The spectrum of benzylidene-aniline has a long tapering end at long wavelengths, analysis of which suggests the presence of a weak band ( $\log \epsilon \sim 2.0$ ) near 360 nm, due to a  $\pi^* + n$  transition [22, 23].

The conjugation of an aromatic system with the azomethine chromophore (having lone-pair electrons) generally shifts the  $\pi^* + n$  band to longer wavelengths and produces a large increase in intensity. Bonnett [24] suggested that an aryl group appears to conjugate effectively when substituted on the carbon atom of the azomethine group, but it may not do so when substituted on the nitrogen atom. Thus, the spectrum of benzylidene-aniline differs in detail from that of stilbene [25], because the N-phenyl group is twisted out from the plane of the rest of the chromophore [24, 26].

A similar conclusion can be drawn in the case of salicylidene derivatives. It is noteworthy that, in the spectrum of salicylidene-n-butylamine (218, 256, 262 and 320 nm,  $\log \epsilon = 4.38, 4.03, 3.90$  and 3.51) (see Fig. 2), the intensity relation of the two maxima of the middle band is reversed



and the halfband width increases. Analysis of the curve gives a weak band at 270 nm ( $\log \epsilon \sim 2.50$ ).

The spectra of the salicylidene-anilines (Fig 3.) dif-

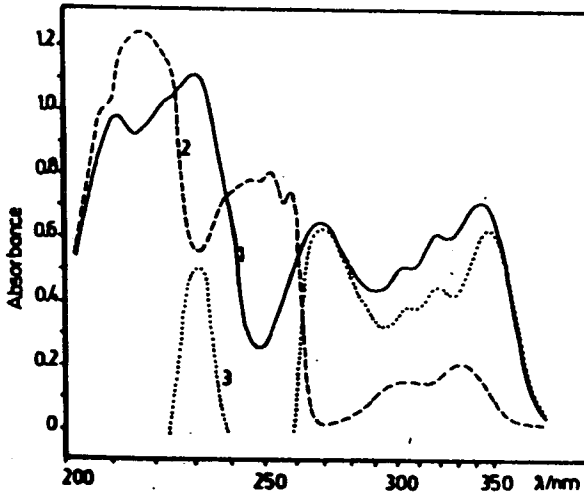


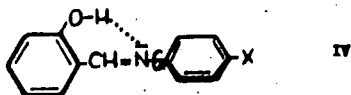
Figure 3.: Spectra of n-hexane solutions. 1: salicylidene-p-toluidine; 2: salicylaldehyde + p-toluidine; 3: (salicylidene-p-toluidine) - (salicylaldehyde + p-toluidine), differential spectrum.

$$c = 5 \cdot 10^{-4} \text{ mol/dm}^3, d = 0.1 \text{ cm}$$

fer completely from those of the components, and also from the sum of the spectra of the components (Fig. 3). The greatest difference can be observed in the range 280-360 nm, resolution of which into gaussian curves results in several bands, and we presume that the weak band ( $f \sim 10^{-4}$ ) in the interval 270-280 nm ( $\log \epsilon \sim 2.60-2.80$ ) is assignable to the

$\pi^* + n$  transition.

It is known [19] that, in general, absorption involving lone-pair electrons moves to higher frequencies if, for example, a hydrogen-bond stabilizes the lone-pair in the ground state. In the case of the salicylidene derivatives, an intramolecular hydrogen-bond is formed (IV) in which the



lone-pair also takes part; consequently, the promotion energy will be increased. The Schiff bases of salicylaldehyde and 2-aminopyridines also display a weak band between 300 and 400 nm, which is probably a  $\pi^* + n$  band [27].

It seems that the N-phenyl group does not appreciably influence the energy of the  $\pi^* + n$  transition. This is understandable, because the N-phenyl ring is twisted out from the plane of the rest of the molecule; consequently, the conjugation between the aromatic ring and the azo-methine linkage is limited and the 4-X substituents studied do not essentially influence the dihedral angle [7]. The probable data on the  $\pi^* + n$  bands of the Schiff bases studied are given in Table II.

Table II

Characteristics on the  $\pi^* \leftarrow n$  bands

Compound	$\lambda/\text{nm}$	$\log \epsilon$
butylidene-n-butylamine	230	~2.30
benzylidene-n-butylamine	300	~2.45
n-butylidene-aniline	320	~2.40
benzylidene-aniline	360	~2.00
salicylidene-n-butylamine	270	~2.60
salicylidene-4-X-aniline	270-290	~2.60-2.80

## References

- [1] Császár, J., et al.: Acta Phys. Chem., Szeged, 25, 129 (1979); 28, 135 (1983).
- [2] Császár, J.: Acta Phys. Chem., Szeged, 27, 47 (1981).
- [3] Chatterjee, K.K., B.E. Douglas: Spectrochim. Acta, 21, 1625 (1965).
- [4] Houlden, S.A., I.G. Csizmadia: Tetrahedron, 25, 1137 (1969).
- [5] Brocklehurst, P.: Tetrahedron, 18, 299 (1962).
- [6] Császár, J., J. Balog: Acta Chim. Hung., Budapest, 87, 321 (1975).
- [7] Császár, J.: Acta Phys. Chem., Szeged, 29, 133 (1983).
- [8] Császár, J., et al.: Acta Phys. Chem., Szeged, 29, 139 (1983); 30, 61 (1984); 31, 729 (1985).
- [9] Holm, R.H., G.W. Everett: Progr. Inorg. Chem., 7, 83 (1966).
- [10] Dudek, G.O., E.P. Dudek: J. Amer. Chem. Soc., 88, 2407 (1966).

- [11] Bakerek, V.: Coll. Czech. Chem. Comm., 33, 994 (1968).
- [12] Császár, J., et al.: Acta Chim. Hung., Budapest, 86, 9, 101 (1975).
- [13] Jaffé, H.H., *M. Orchin: Theory and Application of Ultraviolet Spectroscopy.*, J. Wiley and Sons, New York, 1964.
- [14] Hires, J., J. Balog: Acta Phys. Chem., Szeged, 2, 87 (1956).
- [15] Bonnett, R., N.J. David, J. Hamlin, P. Smith: Chem. Ind., 46, 1836 (1963).
- [16] Mason, S.F.: Quart. Rev., 15, 287 (1961).
- [17] Platt, J.R.: in Radiology Biology., Ed. A. Hollaender, Vol. 3, Chap. 2, McGraw-Hill, New York, 1956.
- [18] Sindman, J.W.: Chem. Rev., 58, 689 (1958).
- [19] Kasha, M.: Discussion Farad. Soc., 9, 14 (1950)
- [20] Scheibe, G.: Ber., 59, 2619 (1926).
- [21] Scheibe, G., F. Felgor, G. Rossler: Ber., 60, 1406 (1927).
- [22] Jaffé, H.H., Si-J. Yeh, R.W. Gardner: J. Mol. Spectr., 2, 120 (1958).
- [23] Smets, G., A. Delvaux: Bull. Soc. Chim. Belge, 56, 106 (1947).
- [24] Bonnett, R.: in the Chemistry of Carbon-Nitrogen Double Bond., Ed. S. Patai, Intersci., New York, 1970.
- [25] Cohen, M.D., Y. Hirshberg and G.M.J. Schmidt: J. Chem. Soc., 2060 (1964).
- [26] Hantzsch, A.: Ber., 23, 2325 (1890).
- [27] Ranganathan, H., T. Ramasini, D. Ramaswamy, M. Santappa: Indian. J. Chem., 25A, 127 (1986).

СРАВНЕНИЕ УФ СПЕКТРОВ АРОМАТИЧЕСКИХ ШИФФОВЫХ ОСНОВАНИЙ И ПРОДУКТОВ ИХ ВОССТАНОВЛЕНИЯ: ВОЗМОЖНОСТЬ ОТНЕСЕНИЯ  $\pi^* \leftarrow n$  ПЕРЕХОДА В АЗОМЕТИНОВОЙ ГРУППЕ

И. Часар

Изучены УФ спектры Шиффовых оснований 4-х-н(2-гидрокси-бензилидено) анилинового типа ( $x = C_2H_5, OC_2H_5, CH_3, OCH_3, H, Cl, Br$ ) и их продуктов восстановления, после действия  $NaNH_4$ . Основное внимание было обращено на явление  $\pi^* \leftarrow n$  перехода характерного для азометиновой группы.

STUDY OF THE SPECTRAL BEHAVIOUR OF MOLECULAR COMPLEXES OF  
PICRIC ACID AND HEXANITROBIPHENYLAMINE WITH SCHIFF BASES  
FORMED FROM SALICYLALDEHYDE AND ALKYL-AMINES, POLYMETHY-  
LENEDIAMINES, SULPHONAMIDES AND AMINOPYRIDINES

By

J. CSÁSZÁR

Institute of General and Physical Chemistry, József Attila University,  
H-6701, Szeged, P.O.B. 105, Hungary

*(Received 9 August 1988)*

Molecular complexes of picric acid and hexanitrobiphenylamine with Schiff bases (SB) derived from salicylaldehyde and alkylamines, polymethylenediamines, sulphonamides and aminopyridines, with formulae SB.A or SB.A<sub>2</sub> (A = acceptor molecule), were prepared and characterized through UV, visible, IR and <sup>1</sup>H NMR spectroscopy. Picric acid and hexanitrobiphenylamine act as acceptor molecules and bind to the aromatic rings of the donors via intermolecular  $\pi - \pi$  charge-transfer interactions.

Pfeiffer [1] suggested that the interactions between the components in a molecular complex could be regarded as interactions between particular force fields to be assigned to certain regions of the molecules. For example, when an aromatic amine is complexed with a polynitrophenol, for instance picric acid, PA, two types of force field must be considered: one type of force field produces an acid-base

interaction (proton transfer, PT), and the other type an electron donor-acceptor interaction (charge transfer, CT).

The preparation of PA complexes through the use of different solvents, and the isomerism of CT-PT complexes, were extensively studied by Matsunaga et al. [2-4]. Issa et al. [5-6] pointed out that, in the molecular complexes of benzylidene derivatives and PA, the occurrence of CT, PT and  $n-\pi$  interactions is possible.

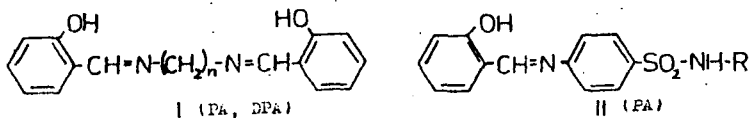
As part of a continuing survey of the spectral characteristics of Schiff bases (SB) [7-10] and of their molecular complexes [11, 12], we have examined the ability of the SB derived from salicylaldehyde with alkylamines, [13], polymethylenediamines [9], sulphonamides [14] and aminopyridines to form molecular complexes with different acceptor molecules. We now report the preparation and the UV, visible, IR and  $^1\text{H}$  NMR spectra of molecular complexes of SB of types I, II, III and IV as donors with PA or hexanitrobiphenyl-amine (dipicrylamine, DPA) as acceptor molecule (see Table I).

### *Experimental*

The SB were synthesized as described previously [13-15]. The complexes were prepared by mixing hot methanolic solutions of donor and acceptor in 1:1 and 1:2 mole ratios. On cooling, crystalline products separated out, which were filtered off and washed with cold ethanol and ether. The m.p.s. and the analytical data on the complexes prepared are listed in Table II. The SB with even numbers of methylene groups form crystalline products with PA more easily and faster, but in the case of longer chains ( $n > 8$ ) no crystal-

Table I

The Schiff bases studied and the numbering of their molecular complexes in the text

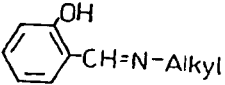
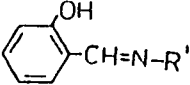


No.	n	Comp.	No.	n	Comp.	No.	R*
<u>1</u>	0	1:1	<u>5</u>	5	1:1	<u>8</u>	-C <sub>6</sub> H <sub>7</sub> N <sub>2</sub>
<u>1a</u>		1:2	<u>5a</u>		1:2	<u>9</u>	-C(O)NH <sub>2</sub>
<u>2</u>	2	1:1	<u>6</u>	6	1:1	<u>10</u>	-C <sub>5</sub> H <sub>5</sub> N <sub>2</sub> O
<u>2a</u>		1:2	<u>6a</u>		1:2	<u>11</u>	-C <sub>6</sub> H <sub>7</sub> N <sub>2</sub>
<u>3</u>	3	1:1	<u>7</u>	8	1:1	<u>12</u>	-C <sub>5</sub> H <sub>5</sub> N <sub>2</sub> O
<u>3a</u>		1:2	<u>7a</u>		1:2	<u>13</u>	-C <sub>6</sub> H <sub>7</sub> N <sub>2</sub> O <sub>2</sub>
<u>4</u>	4	1:1				<u>14</u>	-C <sub>5</sub> H <sub>6</sub> NO
<u>4a</u>		1:2				<u>15</u>	-C <sub>4</sub> H <sub>4</sub> NS

\* The parent sulphonamides: 8: 2-(4'-aminophenylsulphonyl)-amino-4,6-dimethylpyrimidine; 9: (4'-aminophenylsulphonyl)-carbamide; 10: 6-(4'-aminophenylsulphonyl)-amino-3-methoxypyridiazine; 11: 6-(4'-aminophenylsulphonyl)-amino-2,4-dimethylpyrimidine; 12: 2-(4'-aminophenylsulphonyl)-amino-5-methoxypyrimidine; 13: 6-(4'-aminophenylsulphonyl)-amino-2,4-dimethoxypyrimidine; 14: 5-(4'-aminophenylsulphonyl)-amino-3,4-dimethyl-1,2-oxazole; 15: 5-(4'-aminophenylsulphonyl)-amino-3-methyl-1,4-thiazole.



Table I (Continued)

					
III (DPA)		IV (DPA)			
No.	Alkyl	No.	Alkyl	No.	R' **
<u>16</u>	CH <sub>3</sub>	<u>22</u>	n-C <sub>5</sub> H <sub>11</sub>	<u>28</u>	-C <sub>5</sub> H <sub>4</sub> N
<u>17</u>	C <sub>2</sub> H <sub>5</sub>	<u>23</u>	i-C <sub>5</sub> H <sub>11</sub>	<u>29</u>	-C <sub>5</sub> H <sub>4</sub> N
<u>18</u>	n-C <sub>3</sub> H <sub>7</sub>	<u>24</u>	C <sub>6</sub> H <sub>13</sub>	<u>30</u>	-C <sub>5</sub> H <sub>4</sub> N
<u>19</u>	i-C <sub>3</sub> H <sub>7</sub>	<u>25</u>	C <sub>8</sub> H <sub>17</sub>	<u>31</u>	-C <sub>5</sub> H <sub>3</sub> N(CH <sub>3</sub> )
<u>20</u>	n-C <sub>4</sub> H <sub>9</sub>	<u>26</u>	C <sub>10</sub> H <sub>21</sub>	<u>32</u>	-C <sub>5</sub> H <sub>3</sub> N(CH <sub>3</sub> )
<u>21</u>	i-C <sub>4</sub> H <sub>9</sub>	<u>27</u>	C <sub>12</sub> H <sub>25</sub>	<u>33</u>	-C <sub>5</sub> H <sub>3</sub> N(CH <sub>3</sub> )

\*\*

Amines used: 28: 2-aminopyridine; 29: 3-aminopyridine; 30: 4-aminopyridine; 31: 2-amino-3-methylpyridine; 32: 2-amino-4-methylpyridine; 33: 2-amino-5-methylpyridine; 34: 2-amino-6-methylpyridine.

line product can be isolated. The DPA complexes of salicylidene-alkylamines (16-27) were investigated only in solutions prepared with different mole ratios.

The UV and visible spectra were recorded on a SPECORD UV-VIS spectrophotometer in spectroscopically pure solvents at room temperature. The IR measurements were carried out on a ZEISS SPECORD M80 instrument in KBr discs. The <sup>1</sup>H NMR spectra were obtained on a BRUKER FT80 instrument in DMSO-d<sub>6</sub>, using TMS as internal standard\*\*\*.

\*\*\*

The author is grateful to Dr. G. Horváth (CHINOIN) for the <sup>1</sup>H NMR and IR measurements.

Table II

Analytical data on the molecular complexes prepared

No.	Col*	M.P.**	C %		H %	
			Calcd.	Found	Calcd.	Found
<u>1</u>	LY	170 - 173	51.18	51.07	3.12	3.20
<u>1a</u>	LY	193.5 - 194.5	44.71	44.06	2.60	2.33
<u>2</u>	LY	113.5 - 114.0	53.12	52.44	3.85	4.00
<u>2a</u>	LY	170 - 172	46.29	47.82	3.06	2.84
<u>3</u>	O	147 - 149	54.01	53.87	4.14	4.05
<u>3a</u>	LY	177 - 179	47.03	46.77	3.27	3.09
<u>4</u>	O	175 - 176	54.86	54.66	4.41	4.31
<u>4a</u>	LY	195 - 196	47.75	47.51	3.47	3.33
<u>5</u>	O	123.5 - 124.5	55.66	55.33	4.67	4.56
<u>5a</u>	LY	164.5 - 165.5	48.44	48.37	3.67	3.51
<u>6</u>	LY	155 - 156	56.42	56.40	4.92	4.77
<u>6a</u>	LY	175 - 176	49.11	49.01	3.86	3.88
<u>7</u>	LY	153.5 - 154.5	57.83	57.77	5.37	5.31
<u>7a</u>	LY	161 - 162	50.37	49.98	4.23	4.21
<u>8</u>	LY	113 - 114	44.29	44.08	2.88	2.72
<u>9</u>	BY	139 - 140	40.16	39.88	2.46	2.33
<u>10</u>	LY	160 - 161	42.76	41.64	2.63	2.53
<u>11</u>	O	106 - 107	44.29	44.08	2.88	2.58
<u>12</u>	LY	180 - 181	42.76	42.59	2.63	2.55
<u>13</u>	O	74 - 75	42.67	42.55	2.77	2.59
<u>14</u>	O	77 - 78	43.43	43.09	2.79	2.68
<u>15</u>	O	119 - 120	41.88	41.66	2.55	2.52
<u>28</u>	R	177.0 - 177.5	40.16	39.86	1.87	2.01
<u>29</u>	SC	186 - 187	45.32	45.85	2.37	2.50
<u>30</u>	R	199.5 - 200.0	40.16	39.54	1.87	1.94
<u>31</u>	SC	197 - 198	40.75	40.28	2.03	1.96
<u>32</u>	BR	196 - 197		40.33		1.88
<u>33</u>	SC	175 - 176		40.25		1.92
<u>34</u>	SC	186 - 187		39.98		2.00

\* Y: yellow; R: red; SC: scarlet; BR: brownish-red;  
O: orange; LY: lemon-yellow; BY: brownish-yellow

\*\* uncorrected values.

*Results and Discussion*

A) PA complexes 1-2 (1:1) and 1a-7a (1:2). Upon complex formation, the spectra of the SB [15] change considerably (Table III); the 240-320 nm bands become indistinct, and only inflections appear (Fig. 1/2). In the range 350-420 nm,

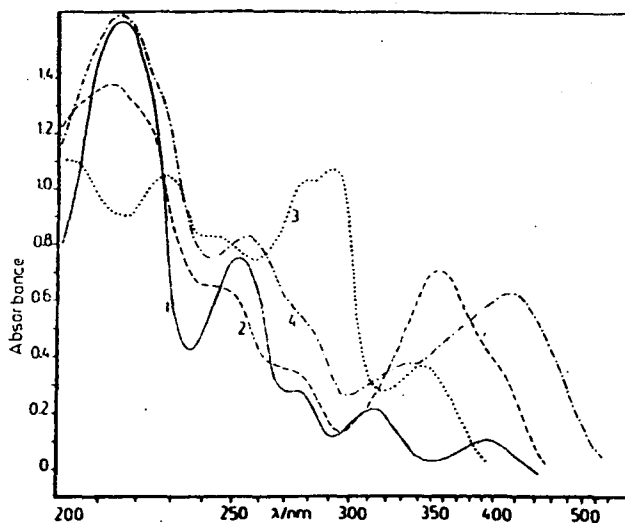


Figure 1.: UV and visible spectra of the SB( $n=5$ ) (1),  $c=2.09 \cdot 10^{-4}$ ; 5a (2),  $c=3.90 \cdot 10^{-4}$ ; 5a in cc sulphuric acid (3),  $c=3.85 \cdot 10^{-4}$ ; the 1:1 DPA complex (4),  $c=2.12 \cdot 10^{-6} \text{ mol/dm}^3$ . Solvent (1, 2, 4): methanol;  $d=0.1 \text{ cm}$ .

a medium-intensity, broad band appears with an inflection on the long-wavelength side. In chloroform (and in other solvents not forming hydrogen-bonds), the spectral struc-

Table III

## Spectral data on the PA complexes

No.	$\lambda/\text{nm}$ and $\log \epsilon$ measured in $\text{CH}_3\text{OH}$					
<u>1</u>	220 (4.63)	~240	-	295 (4.57)	356 (4.61)	~420
<u>1a</u>	220 (4.86)	~240	-	294 (4.73)	354 (4.81)	~420
<u>2</u>	415 (4.69)	~230	257 (4.39)	~280	354 (4.39)	~400
<u>2a</u>	214 (4.75)	~230	252 (4.50)	~280	353 (4.48)	~400
<u>3</u>	216 (4.60)	~230	~245	~280	351 (4.39)	~410
<u>3a</u>	214 (4.72)	~230	~240	~280	352 (4.58)	~410
<u>4</u>	214 (4.82)	~225	253 (4.51)	~278	351 (4.44)	~400
<u>4a</u>	213 (4.79)	~225	~255	274 (4.49)	353 (4.53)	~400
<u>5</u>	214 (4.75)	~225	~250	~280	355 (4.51)	~400
<u>5a</u>	211 (4.73)	~225	-	275 (4.48)	355 (4.63)	~400
<u>6</u>	214 (4.77)	~225	257 (4.46)	274 (4.45)	352 (4.41)	~400
<u>6a</u>	211 (4.83)	~225	-	274 (4.63)	352 (4.64)	~400
<u>7</u>	212 (4.59)	~225	-	274 (4.33)	354 (4.44)	~400
<u>7a</u>	213 (4.79)	~225	-	275 (4.59)	354 (4.66)	~400
<u>8</u>	204 (4.79)	-	~240	273 (4.48)	351 (4.48)	~390
<u>9</u>	~215	-	~250	270 (4.36)	350 (4.20)	~400
<u>10</u>	~210	-	~250	~270	349 (4.33)	~400
<u>11</u>	203 (4.84)	-	254 (4.60)	301 (4.36)	351 (4.39)	~400
<u>12</u>	214 (4.54)	-	~235	271 (4.33)	350 (4.04)	~410
<u>13</u>	~215	-	260 (4.37)	~278	350 (4.09)	~410
<u>14</u>	213 (4.61)	-	~245	271 (4.37)	350 (4.21)	~400
<u>15</u>	~215	-	~245	288 (4.25)	350 (4.28)	~400

ture is similar, but the long-wavelength band is almost symmetrical; the inflection is absent. The spectra of the

complexes with compositions donor/acceptor 1:1 and 1:2 do not differ considerably.

The main IR frequencies of the SB are not changed significantly in their PA complexes; the frequencies of the =NH-group are not detectable, and thus a PT from the OH group of PA to the nitrogen atom of the azomethine group can be excluded. The  $\nu_{\text{CH}}$  bands of the donors shift to higher wavenumbers, indicating a decrease in the  $\pi$ -electron density as a consequence of the intermolecular CT. The  $\nu_{\text{S}}\text{NO}_2$  band of the acceptor shifts to lower wavenumbers (from 1352 to 1325-1340  $\text{cm}^{-1}$ ); the increased  $\pi$ -electron density favours a higher polarization of the nitro group, and accordingly a lower N=O bond order.

We presume that, in the spectra of methanolic solutions of 2-7 and 2a-7a, the range 210-320 nm contains the bands of the  $\pi^* \leftarrow \pi$  transitions of both the donor and acceptor molecules, while the 350 nm band involves the band of PA itself ( $\lambda_{\text{max}} = 350 \text{ nm}$ ,  $\log \epsilon = 4.02$ ), the band of the intermolecular CT, and the band ( $\sim 420 \text{ nm}$ ) of the tautomeric equilibrium system characteristic of SB of this type [9]. It seems that the interaction with PA does not prevent the formation of the hydrogen-bonds within the SB molecule. In contrast with the example described above, the spectra of 1 and 1a are different from those of the other compounds discussed, whereas those of the parent SB and of 1 and 1a are similar (Fig. 2), and do not change in different solvents.

It is interesting that, while the parent SB undergoes hydrolysis relatively rapidly in concentrated sulphuric acid solution, the PA complexes remain almost unchanged during 60-80 min (Fig. 1/3).

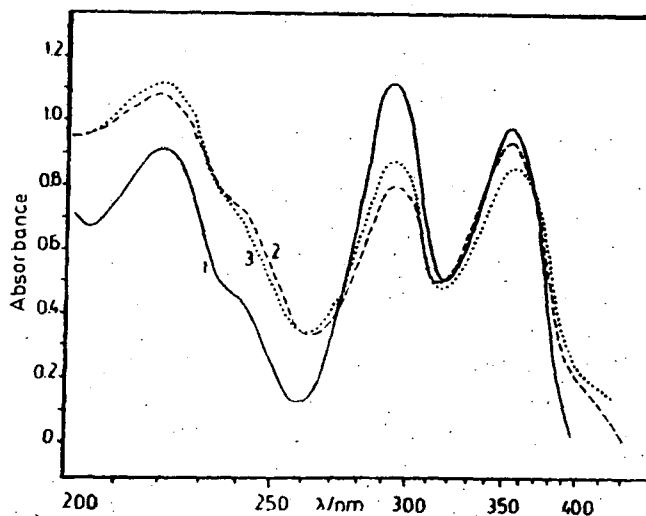


Figure 2.: Spectra of methanolic solutions of the SB( $n=0$ ) (1),  $c=4.2 \cdot 10^{-4}$ ; 1a (2),  $c=4.3 \cdot 10^{-4}$ ; and the 1:1 DPA complex (3),  $c=2.3 \cdot 10^{-4}$  mol/dm<sup>3</sup>;  $d=0.1$  cm.

B) PA complexes 8-15. The spectral structures of the PA complexes (Table III) do not differ fundamentally from that of the corresponding SB [14]; the characteristic 270 nm band is unambiguously observable. In the spectra of the SB, there is a flat part between 280 and 350 nm, with an indistinct band at around 340 nm [14], whereas the spectra of the PA complexes (Figs 3 and 4) display a high-intensity band in this region. The calculated curve and the measured one exhibit a considerable intensity difference, from which we conclude that this range contains bands of different origins, as discussed above. The high-intensity bands below 300 nm result from the  $\pi^* \rightarrow \pi$  transitions of the aromatic systems. It is re-

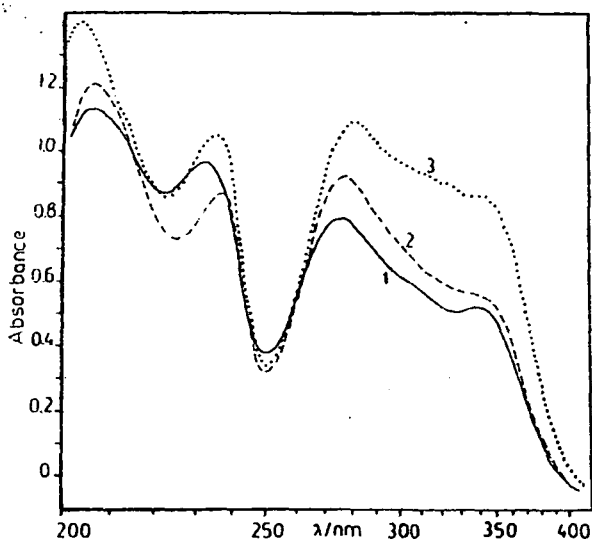


Figure 3.: Spectra of methanolic solutions of 14 (1),  $c=3.8 \cdot 10^{-4}$ ; 9 (2),  $c=6.23 \cdot 10^{-4}$ ; and 15 (3),  $c=5.09 \cdot 10^{-4}$  mol/dm<sup>3</sup>;  $d=0.1$  cm.

markable that the -NH-R heteroaromatic ring scarcely influences the spectra; the complexes of 8 and 9, for example, even when R=H, give totally similar spectra.

In the IR spectra, a broad, medium-intensity band exists, at around  $3000-3100$  cm<sup>-1</sup>, due to the  $\nu$ OH vibration. The strong bands between  $1630$  and  $1660$  cm<sup>-1</sup> correspond to the stretching vibration of the C=N bonds, while there is a strong, broad band between  $1550$  and  $1570$  cm<sup>-1</sup>, which can be assigned as a  $\nu_{as}NO_2$  vibration. If there is some other, for example  $n-\pi$  interaction, two  $\nu_{as}NO_2$  bands appear; one of these is again equal to or greater than the frequency of the

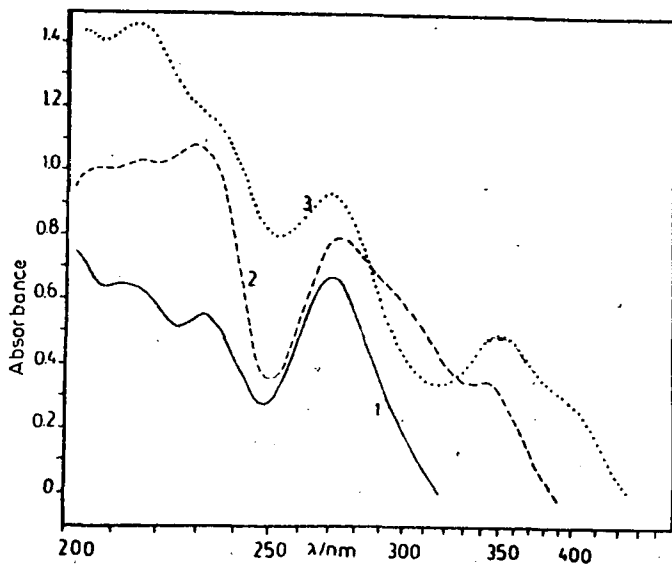


Figure 4.: Spectra of methanolic solutions of the parent sulphonamide of 12 (1),  $c=3.8 \cdot 10^{-4}$ ; the SB (2),  $c=3.9 \cdot 10^{-4}$ ; and 12 (3),  $c=4.4 \cdot 10^{-4}$  mol/dm<sup>3</sup>;  $d=0.1$  cm.

single band of PA, while the second band is located at lower frequencies [16]. The bands of the  $\nu_{as}SO_2$  and  $\nu_sSO_2$  vibrations are also well distinguishable in the range of 1340-1370 and 1150-1170  $cm^{-1}$ , respectively. It can be stated that the IR spectra show differences only in the range of the skeletal vibrations; the other ranges are similar. Unfortunately, the spectra are extremely rich in bands, so a full assignment is difficult.



C) DPA complexes. It has long been known that DPA yields slightly soluble compounds with, for example, quaternary ammonium compounds [17] or different organic bases [e.g. 18, 19], but very few data can be found in the literature on the spectral behaviour of molecular complexes of aromatic SB and DPA.

While the molecular complexes of SB with PA are generally yellow or orange, the complexes of DPA are brick-red, scarlet or violet. From the structure of DPA, it is obvious that donor + acceptor PT is impossible, and thus only CT processes need be taken into account.

Salicylidene-polymethylenediamines (1-7) form red crystalline complexes with compositions 1:1 and 1:2, the spectra of which are very similar to those of the PA complexes (Figs 1/4 and 2/3); the long-wavelength band shifts to approx. 410-420 nm, due to the increased conjugation systems. On the basis of the high similarity of the spectra, it is reasonable to assume that the PA and DPA complexes have similar structures, and similar excitation processes play important roles in their spectra.

The salicylidene-alkylamines (16-27) also form molecular complexes with DPA in chloroform or methanolic solution, with composition 1:1. In this series, all the spectra display a high similarity to each other; for a typical example, see Fig. 5. The spectra of these compounds are complicated superpositions of the spectra of the components: the long-wavelength band also contains the band assigned to the CT processes, in which the aldehyde ring of the SB obviously takes part in the interaction.

Molecular complexes 28-30 exhibit different spectral structures. 28 shows two bands (295-310 and 380-430 nm); the latter one has the higher intensity. In the case of 29,

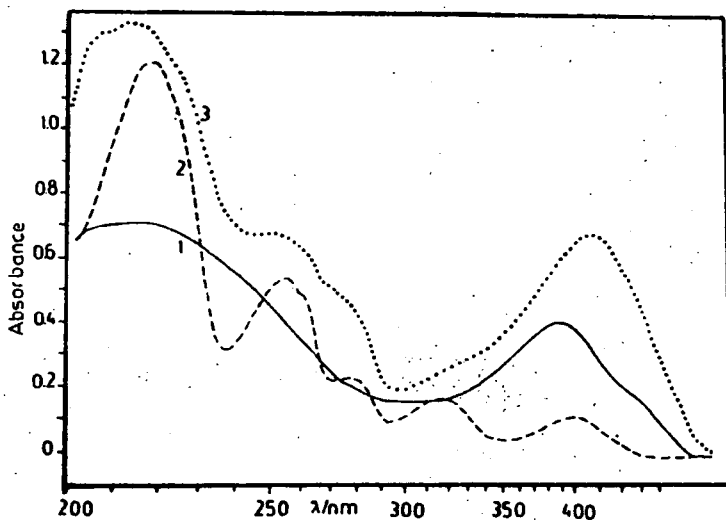


Figure 5.: UV and visible spectra measured in methanol  
 (1) DPA,  $c=3.19 \cdot 10^{-4}$ ; (2) SB of 26,  
 $c=2.30 \cdot 10^{-4}$ ; (3) SB+DPA,  $c_{SB}=1.9 \cdot 10^{-4}$ ,  
 $c_{DPA}=2.15 \cdot 10^{-4}$  mol/dm<sup>3</sup>;  $d=0.1$  cm.

the bands lie closer together (340-360 and 410-430 nm) and they have comparable extinction coefficients, while in the spectra of 30, only one, high-intensity, broad band exists (Table IV, Fig 6).

The visible band is in every case broad and asymmetric. Accordingly, we presume that this band contains not only the 385 nm band of DPA, but also the band which corresponds to the  $\pi - \pi$  CT. An important solvent effect is observable in the spectra of 29-34 (see Tables IV and V), but no relationship can be found between the spectral changes and the

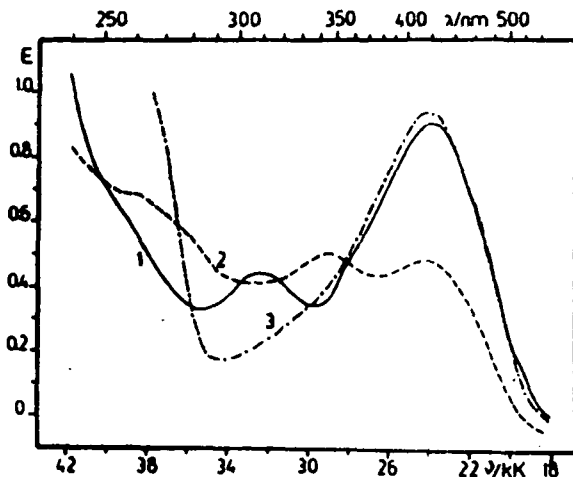


Figure 6.: Spectra measured in methanol. (1) 28,  $c=1.11 \cdot 10^{-4}$ ; (2) 29,  $c=1.30 \cdot 10^{-4}$ ; (3) 30,  $c=1.30 \cdot 10^{-4}$  mol/dm<sup>3</sup>;  $d=0.1$  cm.

solvent characteristics. The solution spectra do not rigorously obey the Beer law, so we assume that an equilibrium system is formed in solution. In the reflection spectra of 28-30, no band appears in the visible; only a well-defined inflection is observed at around 400 nm.

Selected <sup>1</sup>H NMR and IR data on 28-30 are presented in Table IV; partial spectra are shown in Fig. 7. A comparison between the NMR spectra of the studied complexes and those of the components reveals that the signals of the donors and the acceptor are generally shifted to higher and lower  $\delta$ (ppm) values, respectively. The shifts of the signals due to the pyridine protons are higher, which supports the as-

Table IV

UV, visible ( $\lambda_{\max}$ /nm and  $\log \epsilon$ ),  $^1\text{H}$  NMR and IR ( $\text{cm}^{-1}$ )  
spectral data on complexes 28-30

Solv.	28		29		30
MeOH	310 (4.62)	421 (4.92)	348 (4.36)	417 (4.34)	419 (4.86)
$\text{CHCl}_3$	~280	~460	349 <sup>a)</sup>	~400	415 <sup>a)</sup>
$\text{CH}_3\text{CN}$	298 (4.43)	423 (4.84)	354 (4.44)	420 (4.43)	438 (4.82)
DMSO	309 (4.70)	430 (4.93)	340 (4.32)	434 (4.32)	438 (4.82)
Acid	303 (4.65)	380 (4.58)	336 <sup>a)</sup>	~280	380 <sup>a)</sup>
Base	300 (4.47)	422 (4.85)	283 (4.42)	406 (4.67)	420 (4.75)

Assignments

$\delta\text{CHN}$	8.80	8.80	8.80
$\delta\text{CH}(\text{py-ring})$	7.90 <sup>b)</sup>	7.68 <sup>b)</sup>	8.08 <sup>b)</sup>
$\delta\text{CH}(\text{ald-ring})$	6.95 <sup>b)</sup>	7.06 <sup>b)</sup>	6.86 <sup>b)</sup>
$\nu\text{NH}$	3100m	3090m	3160m
$\nu\text{C=N}$	1668s	1625s	1650s
$\nu_{\text{as}}\text{NO}_2$	1588s	1560s	1585s
$\nu_{\text{s}}\text{NO}_2$	1285s	1305s <sup>c)</sup>	1305s <sup>c)</sup>
$\gamma\text{C-N(H)}$	1166m	1170m	1160m
$\gamma_{\text{CH}}$	{ 908m	{ 908m	{ 907m
	{ 767m	{ 764m	{ 765m
	{ 738m	{ 740m	{ 738m
	{ 718m	{ 718m	{ 720m

a) very poorly soluble; b) the values denote the main frequencies of the multiplets; c) broad complex band

Table V

Spectral data on molecular complexes 31-34

No.	Solv.	$\lambda/\text{nm}$ and $\log \epsilon$		
<u>31</u>	MeOH	315 (4.46)	-	422 (4.74)
	CHCl <sub>3</sub>	~280	389 (4.42)	~440
	CH <sub>3</sub> CN	304 (4.32)	-	426 (4.72)
<u>32</u>	MeOH	318 (4.41)	-	420 (4.73)
	CHCl <sub>3</sub>	~280	385 (4.33)	~460
	CH <sub>3</sub> CN	313 (4.34)	-	425 (4.79)
<u>33</u>	MeOH	311 (4.68)	-	420 (5.02)
	CHCl <sub>3</sub>	~280	380 <sup>a)</sup>	~470
	CH <sub>3</sub> CN	302 (4.26)	-	425 (4.72)
<u>34</u>	MeOH	261 (4.72)	350 (4.59)	420 (4.58)
	CHCl <sub>3</sub>	278 (4.78)	350 (4.66)	~390
	CH <sub>3</sub> CN	273 (4.69)	347 (4.63)	423 (4.60)

a) very low solubility

sumption that the pyridine ring is the donating system in the CT interaction. In the case of the parent SB, the two overlapping band systems of the aldehyde and pyridine ring protons lie between 6.7 and 8.1 ppm, while in the spectra of the CT complexes, the two band systems are separated by about 0.8-1.2 ppm.

As a result of the  $\pi - \pi$  interactions, the characteristic IR frequencies of both the donors and the acceptor change. The sharp  $\nu_{\text{NH}}$  frequency of DPA appears at  $3095 \text{ cm}^{-1}$ ;

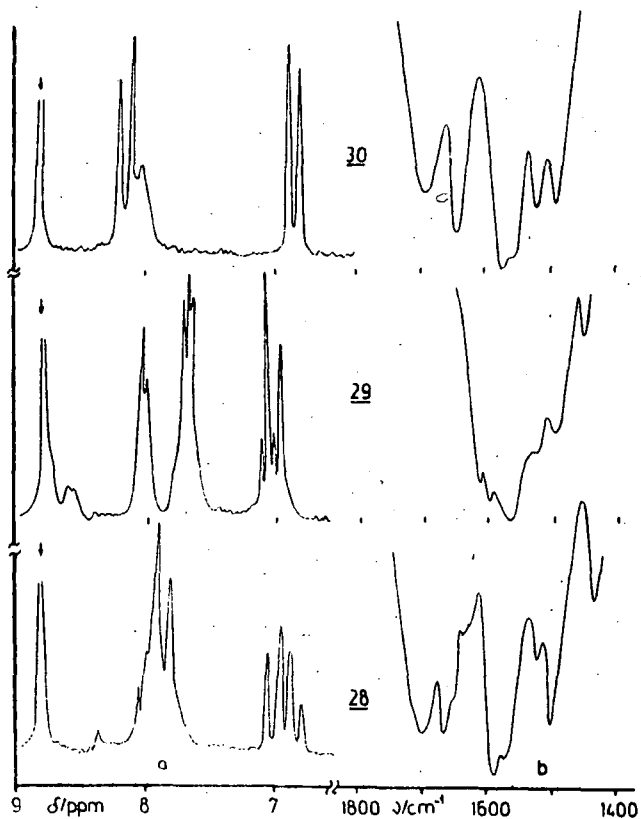


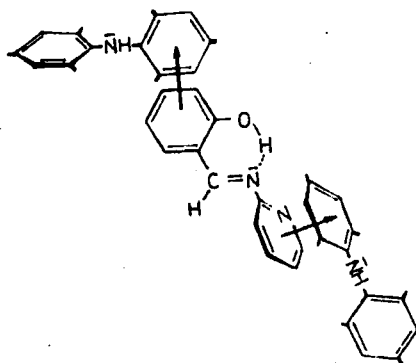
Figure 7.: Partial  $^1\text{H}$  NMR ( $\delta/\text{ppm}$ ) (a) and IR ( $\nu/\text{cm}^{-1}$ ) (b) spectra of DPA complexes 28, 29 and 30.

in the spectra of the complexes it is found at around  $3090\text{--}3200\text{ cm}^{-1}$ . The  $\nu_{\text{as}}\text{NO}_2$  band becomes broader and shows some splitting, indicating a higher differentiation of the

energy states of the nitro groups in the complexes than that in free DPA. A similar change may be observed for the  $\nu_{\text{S}} \text{NO}_2$  bands. The  $\nu_{\text{C}=\text{N}}$  band shifts toward higher wavenumbers as compared to the parent SB molecules. In the range  $700\text{--}910 \text{ cm}^{-1}$ , several bands are observed that are due to the  $\gamma_{\text{CH}}$  vibrations of the different aromatic rings. The  $\gamma_{\text{CH}}$  bands of the donors shift to higher wavenumbers, which is a criterion for a CT interaction of  $\pi - \pi$  type [16, 20]. On the other hand, the  $\gamma_{\text{CH}}$  bands of the pyridine ring exhibit higher shifts in comparison to those of the benzal ring, indicating similarly that the CT takes place between the pyridine ring and the acceptor molecule.

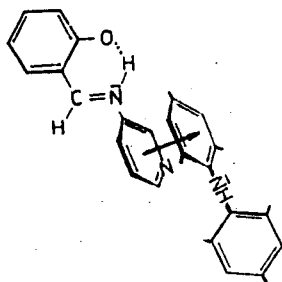
Issa et al. [21] consider that, in the case of benzyldene-aniline derivatives, the aniline ring is the centre primarily contributing to the intermolecular CT interaction; however, in the case of the donor:acceptor 1:2 complexes, the aldehyde ring also takes part in the complex formation. Considering the analytical data and the experimental results, in the case of salicylidene-polymethylenediamines (1-7) and salicylidene-sulphonamide derivatives (8-15), 1:1 + 1:2 and 1:2 complexes are formed, respectively. Since the SB studied are weak electron-donors and PA is a weak acceptor, the resulting CT complex may be expected to be non-ionic. The IR data suggested that the formation of the intramolecular six-membered ring [22, 23] prevents the intermolecular PT; and since the nitrogen lone pair blocks this, the  $n - \pi$  interaction is also improbable; the studied complexes are formed only via an intermolecular CT interaction.

With DPA, 16-27 and 29 form 1:1 complexes, while 28-34 yield 1:2 complexes (not 29). We presume that both the aldehyde and pyridine rings take part in the 1:2 complex formation (Structure V), while in the case of 29 the interac-



V

tion occurs only between the pyridine ring and the aromatic system of the acceptor (Structure VI). However, the dif-



VI



ferent behaviour of 29 is difficult interpret. Saito and Matsunaga [3] have reported amine-PA 1:2 molecular complexes, in which half of the amine molecules act as proton-acceptors, while the other half participate in CT interactions with the picrate ion; i.e. one of the two PA may be a proton-donor, and the other an electron-acceptor. In this case, the IR spectra show the  $\nu\text{-}\overset{\oplus}{\text{N}}\text{H}_3$  band in the range 2500-300  $\text{cm}^{-1}$ . We have no experimental data suggesting the simultaneous operation of CT and PT and/or  $n - \pi$  interactions. It is very difficult to interpret the real structures of these molecular complexes, because strong steric inhibition influences the conformations of both the donor and acceptor molecules.

It is very important to note that it is possible to prepare molecular complexes with different compositions from similar donors and acceptors, depending on the experimental circumstances (temperature, solvent, etc); this problem requires still further investigations.

#### References

- [1] Pfeiffer, P.: "Organische Molekülverbindungen", 2. Aufl., Vlg. von P. Enke, 1927., p. 341-346.
- [2] Saito, G., Y. Matsunaga: Bull. Chem. Soc. Japan, 46, 714 (1973).
- [3] Inoue, N., Y. Matsunaga: Bull. Chem. Soc. Japan, 46, 3345 (1973).
- [4] Saito, G., A. Matsunaga: Bull. Chem. Soc. Japan, 47, 1020 (1974).
- [5] Hindawey, A.M., Y.M. Issa, R.M. Issa, H.F. Rizk: Acta Chim.Hung., Budapest, 112, 415 (1983).

- [6] Issa, R.M., S.M. Abu-El-Wafa, M. Gaber, El-H.A. Mohamed: *Acta Chim. Hung.*, Budapest, 118, 179 (1985).
- [7] Charette, J., G. Falthansl, Ph. Teyssie: *Spectrochim. Acta*, 20, 597 (1964).
- [8] Chatterjee, K.K., B.E. Douglas: *Spectrochim. Acta*, 21, 1625 (1965).
- [9] Császár, J., J. Balog, A. Makáry: *Acta Phys. Chem.*, Szeged, 24 473 (1978) and references therein
- [10] Kiss, A., M. Révész, J. Császár, M.I. Bán: *Acta Chim. Hung.*, Budapest, 102, 179 (1979).
- [11] Issa, R.M., N. Gaber, A.L. El-Ansary, H.F. Rizk: *Bull. Soc. Chim. France*, 173 (1985).
- [12] Császár, J.: *Acta Phys. Chem.*, Szeged, in press
- [13] Szabó, T., J. Császár: *Magyar Kémiai Folyóirat*, 83, 21 (1977).
- [14] Császár, J., J. Morvay: *Acta Pharm. Hung.*, 53, 121 (1983).
- [15] Császár, J.: *Acta Phys. Chem.*, Szeged, 28, 135 (1982).
- [16] Kross, R.D., V.A. Fasse: *J. Amer. Chem. Soc.*, 79, 38 (1957).
- [17] Ackerman, D., H. Maner: *Z. physik. Chem.*, 279, 114 (1943).
- [18] Kertes, S.: *Anal. Chim. Acta*, 15, 73 (1956).
- [19] Kertes, S., V. Kertes: *Anal. Chim. Acta*, 15, 154 (1956).
- [20] Issa, Y.M. et al.: *J. Indian Chem. Soc.*, LVII, 216 (1980).
- [21] Dessouki, H.A., R.M. Issa, E.E. Hossani: *Acta Chim. Hung.*, Budapest, in press
- [22] Császár, J.: *Acta Phys. Chem.*, Szeged, 29, 139 (1983).
- [23] Császár, J., M.N. Bizony: *Acta Phys. Chem.*, Szeged, 31, 729 (1985).

ИЗУЧЕНИЕ СПЕКТРАЛЬНЫХ СВОЙСТВ МОЛЕКУЛЯРНЫХ КОМПЛЕКСОВ ШИФФОВЫХ ОСНОВАНИЙ ОБРАЗОВАННЫХ ИЗ САЛИЦИЛОВОГО АЛЬДЕГИДА И АЛКИЛАМИНОВ, ПОЛИМЕТИЛЕНДИАМИНОВ, СУЛЬФОНАМИДОВ И ПИРИДИНОВ С ПИКРИЛОВОЙ КИСЛОТОЙ И ГЕКСАНИТРОБИФЕНИЛАМИНОМ

И. Часар

Синтезированы и характеризованы с помощью УФ, видимой, ИК и  $^1\text{H}$  ЯМр спектроскопии Шиффовые основания (SV) комплексов пикриловой кислоты и гексанитробифениламина, производных салицилового альдегида и алкиламинов, полиметиленодиаминов и аминопиридинов состава  $\text{SV}\cdot\text{A}$  и/или  $\text{SV}\cdot\text{A}_2$  (где А молекула акцептора). Пикриловая кислота и гексанитробифениламин действуют как акцепторы молекул и связываются к ароматическим кольцам доноров путем межмолекулярного взаимодействия п-п электронного переноса заряда.

SOLVENT EFFECT IN THE FORMATION OF SCHIFF BASES

By

P. NAGY AND R. HERZFELD

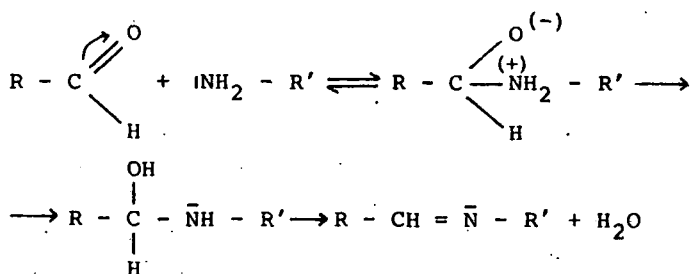
Department of Chemistry, Juhász Gyula Teachers' Training  
College, P. O. Box 396, H-6701 Szeged, Hungary

(Received 30th June, 1988)

The formation of substituted N-(benzylidene)anilines was studied in various solvent mixtures. For compounds containing an OH group in the o- or p-position on the aldehyde ring, good correlations were found between  $\log k$  and the  $E_T^N$  and  $B_{KT}$  values of the solvent mixtures, and between  $\log k$  and the activity coefficient of the more polar solvent component.

*Introduction*

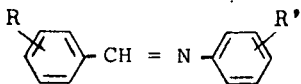
Since Schiff bases are of importance from both theoretical and practical aspects, they have been studied widely. The condensation of aromatic aldehydes and aromatic amines is particularly suitable for the kinetic study of their formation. Kresze and his coworkers [1-3] reported that the mechanism of the kinetically second order process is as follows:



On the basis of this mechanism, it can be expected, that the reaction will be accelerated by any factor which reduces the electron density on the carbonyl carbon atom or increases the electron density on the nitrogen atom. This was earlier confirmed by studies of the effects of the substituents on the aldehyde and amine components [4, 5]. Previous solvent effect results also accord fully with the presumed mechanism [6]. The present paper reports on a study of the rates of formation of some Schiff bases as functions of the acidity and basicity parameters ( $E_T^N$  and  $B_{KT}$ ) of various solvent mixtures and the activity coefficients of the solvent components. This study was intended to clarify details of the solvent effect and the connection between the solvent effect and the substituents. This method has already been applied with good results in investigations of the amine exchange and hydrolysis of Schiff bases [7, 8].

#### *Experimental*

The formations of the following Schiff bases were studied:



<u>1</u>	R = 2-OH,	R' = H
<u>2</u>	R = 2-OH,	R' = 4-CH <sub>3</sub>
<u>3</u>	R = 2-OH,	R' = 4-OCH <sub>3</sub>
<u>4</u>	R = 4-OH,	R' = 4-OCH <sub>3</sub>
<u>5</u>	R = 4-CH <sub>3</sub> ,	R' = 4-CH <sub>3</sub>
<u>6</u>	R = 4-OCH <sub>3</sub> ,	R' = 4-CH <sub>3</sub>

The Schiff bases, aldehydes and amines used for the kinetic measurements were purified by recrystallization or distillation, and their purities were then checked via melting point and boiling point measurements and determination of the absorption curves. The organic solvents applied were purified by means of the methods customary in spectroscopy, and were carefully freed from water. Bidistilled water was used to prepare the alcohol-water solvent mixtures. The reactants were used in  $10^{-3}$ - $10^{-2}$  mol/dm<sup>3</sup> concentration and the reactions were followed spectrophotometrically at 298 K. The rate constants dm<sup>3</sup>.mol<sup>-1</sup>.min<sup>-1</sup> were calculated for second-order reactions. For mixtures containing water, the reverse reaction (hydrolysis) was also taken into consideration.

The acidities of the solvents were characterized in terms of the Reichard parameter  $E_T^N$  [9], and their basicities in terms of the modified Kamlet-Taft parameter  $B_{KT}$  [10, 11]. These parameters were determined earlier [12].

*Results and discussion*

Rate constants determined in various solvent mixtures are given in Tables I-III, which list the  $E_T^N$  and  $B_{KT}$  values of the solvent mixtures, and the activity coefficients ( $\gamma$ ) of one or both components.

Similarly as in investigations of the amine exchange and hydrolysis of Schiff bases [7, 8], the following equation was applied to describe the correlation between the rate constant and the solvent parameters:

$$\log k = b_1 E_T^N + b_2 B_{KT} + a \quad (1)$$

The data in Tables I-III were employed with the method of least squares to determine the constants ( $b_1$ ,  $b_2$  and  $a$ ) in Eq. (1), and the multiple correlation coefficient ( $R$ ) was calculated. For a better comparison of the effects of acidity and basicity, the regression coefficients  $b_1$  and  $b_2$  were converted to beta coefficients  $\beta_1$  and  $\beta_2$ , these were normalized [18, 7], and the distribution of the effects of acidity and basicity ( $\beta'_1$  and  $\beta'_2$ ) was obtained in percentages for the reaction in question. The calculated values are listed in Table IV.

Similarly as in investigations of amine exchange [19], the following relationship was applied to characterize the connection between the rate of formation and the composition of the solvent mixture:

$$\log k = x_1 \log k_1^* + x_2 \log k_2^* + Bx_1x_2 \quad (2)$$

Table I

Rates of formation of Schiff bases (1-6) in ethanol(1)-benzene(2) solvent mixture

$T = 298 \text{ K}$

$x_1$	$\gamma_1$ [13]	$\gamma_2$ [13]	$E_T^N$ [12]	$B_{KT}$ [12]	log k + 4					
					<u>1</u>	<u>2</u>	<u>3</u>	<u>4</u>	<u>5</u>	<u>6</u>
0.000	-	1.00	0.127	0.08	0.477	0.869	1.204	-	0.556	0.146
0.145	3.70	1.12	0.428	0.34	2.079	2.462	2.875	-	0.653	0.301
0.276	2.25	1.29	0.470	0.50	2.352	2.748	3.176	1.720	0.752	0.447
0.395	1.71	1.45	0.501	0.56	2.562	2.929	3.326	1.879	0.851	0.580
0.604	1.25	2.06	0.548	0.64	2.816	3.193	3.577	2.025	1.041	0.799
0.781	1.06	2.80	0.584	0.70	2.997	3.377	3.769	2.312	1.243	1.013
0.932	1.02	3.92	0.633	0.77	3.173	3.556	3.929	2.596	1.562	1.255
1.000	1.00	-	0.655	0.78	3.255	3.638	4.009	2.734	1.785	1.398



Table II

Rates of formation of Schiff bases (1-3) in ethanol  
(1)-acetone.(2) solvent mixture

$T = 298 \text{ K}$

$x_1$	$\gamma_1$ [15]	$E_T^N$ [14]	$B_{KT}$ [14]	$\log k + 4$		
				<u>1</u>	<u>2</u>	<u>3</u>
0.000	-	0.355	0.54	1.114	1.591	1.875
0.123	1.67	0.537	0.55	1.544	1.993	2.398
0.240	2.52	0.580	0.56	1.836	2.305	2.663
0.352	1.40	0.610	0.58	2.009	2.484	2.863
0.558	1.21	0.634	0.61	2.336	2.794	3.188
0.746	1.10	0.643	0.65	2.653	3.117	3.477
0.920	1.03	0.647	0.70	3.045	3.455	3.813
1.000	1.00	0.650	0.77	3.255	3.638	4.009

B values were calculated from the data in Tables I-III, and a study was made as to whether the relationship established for amine exchange [19] was also valid in this case:

$$B = b \gamma_1 + a \quad (3)$$

Values of  $a$  and  $b$  calculated with the method of least squares for the reactions in question, together with the correlation coefficients ( $r$ ), are to be found in Table V.

Table III

Rates of formation of *N*-(2-hydroxybenzylidene)4'-methyl-aniline in water(1)-methanol(2) solvent mixture

$T = 298 \text{ K}$

$x_1$	$\gamma_1$ [17]	$E_T^N$ [16]	$B_{KT}$ [16]	$\log k + 1$
0.000	-	0.77	0.62	0.806
0.195	1.19	0.78	0.54	0.991
0.350	1.14	0.79	0.55	1.176
0.477	1.06	0.81	0.53	1.346
0.584	0.97	0.82	0.50	1.519
0.756	0.83	0.86	0.39	1.833
0.830	0.78	0.89	0.34	2.000
1.000	1.00	1.00	0.19	2.450*

\* extrapolated value

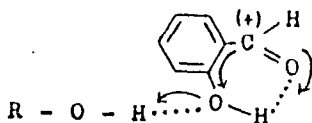
The data in Table IV reveal that Eq. (1) satisfactorily describes the solvent effect in the formation of Schiff bases (1-4) which contain an OH group in the o- or p-position on the aldehyde ring. For the 2-hydroxy derivatives (1-3) in ethanol-benzene, the rate of formation is decisively (94-96 %) influenced by the acidity of the solvent. This can be interpreted in that the OH group in the o-position is intramolecularly hydrogen-bonded here too, and thus the alcohol molecules can interact with it only as hydrogen donors. On the other hand, this interaction greatly increases the positiveness of the azomethine carbon atom and hence the rate

Table IV

Application of equation (1) to the formation of Schiff bases in different solvent mixtures

Solvent mixture	Schiff base	$b_1$	$b_2$	a	$\beta'_1$ (%)	$\beta'_2$ (%)	n	R
ethanol- -benzene	<u>1</u>	5.093	0.193	-4.152	94.87	5.13	8	0.9984
	<u>2</u>	5.061	0.201	-3.759	94.64	5.36	8	0.9986
	<u>3</u>	5.631	-0.162	-3.456	96.04	3.96	8	0.9976
	<u>4</u>	8.967	-2.229	-5.389	72.12	27.88	8	0.9954
	<u>5</u>	-2.066	3.014	-3.572	32.44	67.56	8	0.8785
	<u>6</u>	-2.125	3.197	-3.956	31.77	68.23	8	0.9336
ethanol- -acetone	<u>1</u>	2.829	6.372	-7.373	35.22	64.78	8	0.9934
	<u>2</u>	2.887	5.955	-6.701	37.25	62.75	8	0.9915
	<u>3</u>	3.272	5.723	-6.417	41.19	58.81	8	0.9944
water- -methanol	<u>2</u>	9.153	-0.264	-6.967	93.98	6.02	7	0.9820

of the reaction.



(The interaction between the oxo group and the alcohol can be neglected in comparison with this, but the rate of the reaction is several orders lower in the absence of the 2OH group.) For the 4-hydroxy derivative, the acidity function

Table V

*Application of equation (3) to the formation of Schiff bases in different solvent mixtures*

Solvent mixture	Schiff base	b	a	n	r
ethanol-benzene	<u>1</u>	2.911	-1.016	6	0.9985
	<u>2</u>	2.901	-1.037	6	0.9987
	<u>3</u>	3.089	-1.123	6	0.9986
	<u>5</u>	0.420	-1.943	6	0.7074
	<u>6</u>	0.195	-0.805	6	0.7093
ethanol-acetone	<u>1</u>	3.261	-3.879	6	0.9983
	<u>2</u>	2.669	-2.969	6	0.9934
	<u>3</u>	4.004	-4.431	6	0.9922
water-methanol	<u>2</u>	0.840	-1.859	6	0.9950

of the solvent decreases and its basicity function increases, and the latter hinders the reaction ( $b_2 < 0$ ). The reason for this is probably that alcohol molecules can interact with the OH group in the p-position either as H-donors or as H-acceptors. However, the latter hydrogen-bond decreases the positiveness of the azomethine carbon atom and hence does not promote the reaction.

Naturally, in the examined reactions the interaction between the amine component and the solvent must also be taken into account. The alcohol molecules can form hydrogen-bonds by reacting as either H-donors or H-acceptors with the amino groups, with resulting opposite influences on the nucleophilic nature of the nitrogen atom. Since the

$\text{-O-H}\cdots\cdots\text{N}\leftarrow$  bond is the stronger, the acidity of the solvent can be the more important from the aspect of formation of the Schiff base, hindering the reaction. However, this effect is unimportant if the aldehyde molecules contain OH groups in the o- or p-position, because the rate-increasing effects of these are considerably higher.

The situation changes if the aldehyde component does not contain an OH group in the o- or p-position. In this case the rate of the reaction is considerably lower and thus the importance of the effect of the hydrogen-bond formed with the oxo or amino group increases. However, the acidity of the solvent influences the reactivities of the aldehyde and amine components in opposite ways. This presumably explains why Eq. (1) yields a very poor correlation for compounds 5 and 6 ( $R = 0.8785$  and  $R = 0.9336$ ).

There are very good correlations for compounds 1-3 in ethanol-acetone, but the effect of the acidity of the solvent greatly decreases and the effect of its basicity increases. In our opinion this is caused by hydrogen-bond formation between ethanol and acetone or between amine and acetone. The former hinders the interaction between ethanol and aldehyde, but the latter increases the electron density on the amine-nitrogen and hence the rate of the reaction. In water-methanol, the acidity of the solvent also has a decisive role.

For the formation of Schiff bases (1-3) which contain an OH group in the o-position on the aldehyde molecule, a very good correlation was found with both Eq. (2) and Eq. (3) (Table V), similarly as in the amine exchange of Schiff bases [19]. However, when there are  $\text{-CH}_3$  or  $\text{-OCH}_3$  substituents instead of  $\text{-OH}$  in the molecule, the correlation is very bad. It is interesting that for these compounds  $B < 0$

in Eq. (2), as  $\log k$  measured in the mixture is lower than would follow from the additivity; each solvent component mutually "spoils" the effect of the other. For compounds 1-3,  $B$  is positive; in the mixture  $\log k$  is higher than corresponds to additivity. This is illustrated in Figures 1 and 2.

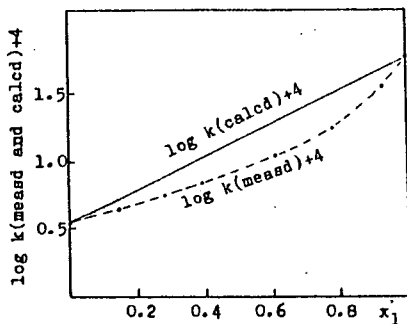


Figure 1.: Deviation of the formation rate of compound 5 from the additivity in ethanol-benzene solvent mixture

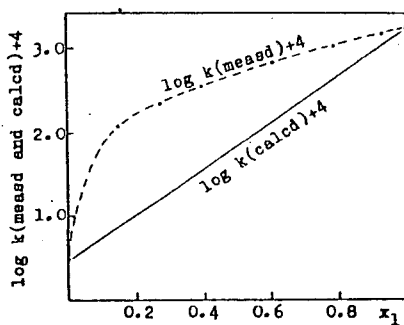


Figure 2.: Deviation of the formation rate of compound 1 from the additivity in ethanol-benzene solvent mixture

In our opinion the explanation of the above finding is as follows: since the association of ethanol molecules decreases in ethanol-benzene, the number of "free" alcohol molecules will be comparatively higher. In the formation of compound 1, these molecules form a hydrogen-bond with the OH group of the aldehyde, thereby greatly increasing the rate of the reaction, to a higher degree than corresponds to additivity. On the other hand, there is no chance of this with compound 5. Accordingly, the rate-reducing effect of the interaction between the amine-nitrogen and the alcohol molecules makes itself felt, and  $\log k$  will be lower than the additive value. In this respect, for compounds 5 and 6 the B values in Eq. (2) decrease linearly with the activity coefficient of benzene; relationship (3) does not express a good correlation with  $\gamma_1$ , but with  $\gamma_2$  ( $b < 0$  and  $r = 0.9979$  and  $0.9981$  for 5 and 6, respectively).

The reported results demonstrate that the aldehyde substituent significantly influences the solvent effect in the examined process.

#### References

- [1] Kresze, G., H. Manthey: Z. Elektrochem. Ber. Bunsenges. Physik Chem. 58, 118 (1954)
- [2] Kresze, G., H. Goetz: Z. Naturforsch. 7., 376 (1955).
- [3] Kresze, G., K. Becker: Z. Naturforsch. 12, 45 (1957).
- [4] Nagy, P., Zs. Molnár: Szegedi Tanárképző Főisk. Tud. Közl. 145 (1966).
- [5] Nagy, P.: Szegedi Tanárképző Főisk. Tud. Közl. 153 (1966).
- [6] Nagy, P.: Szegedi Tanárképző Főisk. Tud. Közl. 61 (1967).

- [7] *Nagy, P., R. Herzfeld: Acta Phys. et Chem. Szeged, 32, 33 (1986).*
- [8] *Nagy, P., R. Herzfeld: Szegedi Tanárképző Főisk. Tud. Közl. in press*
- [9] *Reichardt, C., E. Harbusch-Görnert: Liebigs. Ann. Chem. 721 (1983).*
- [10] *Kamlet, M.J., R.W. Taft: J. Amer. Chem. Soc. 98, 377 (1977).*
- [11] *Krygowski, T.M., E. Milczarek, P.K. Wrona: J. Chem. Soc. Perkin Trans II. 1563 (1980).*
- [12] *Nagy, P., R. Herzfeld: Acta Phys. et Chem. Szeged, 31, 735 (1985).*
- [13] *Nagy, L., G. Schay: Magyar. Kém. Folyóirat, 70, 33 (1964).*
- [14] *Nagy, P., R. Herzfeld: Acta Phys. et Chem. Szeged, 33, 53 (1987).*
- [15] *Landolt-Börnstein: 6th ed., Col. 2. Part 2/a, p. 561.*
- [16] *Krygowski, T.M., P.K. Wrona, U. Zielkowska: Tetrahedron, 41, 4519 (1985).*
- [17] "International Critical Tables", Vol. 3. p. 290, Mc.Graw-Hill.
- [18] *Ezekiel, M., K.A. Fox: "Methods of Correlation and Regression Analysis". 3rd ed., Wiley, New York, 1959.*
- [19] *Nagy, P.: Acta Chim. Hung. 112, 461 (1983).*



ВЛИЯНИЕ ПРИРОДЫ РАСТВОРИТЕЛЕЙ НА  
ОБРАЗОВАНИЕ ОСНОВАНИЙ ШИФФА

П. Надь и Р. Херцфельд

Авторами исследовано образование замещенных  $n$ -(бензиден) анилинов. Для соединений содержащих OH группу в орто или пара положении на альдегидном кольце. Хорошая корреляция найдена между  $lg k$  и  $E_T^N$ ,  $v_{KT}$ , а также коэффициентом активности более полярного компонента смеси.

ELECTRODIC PROCESSES OF DERIVATIVES OF 2,2,4,4 - TETRAMETHYLPENTANE ON STATIONARY SOLID ELECTRODES. I. CYCLIC VOLTAMMETRY OF 3-HYDRAZONES OF 2,2,4,4-TETRAMETHYLPENTANE

By

H. SCHOLL\* AND P. KRZYCZMONIK

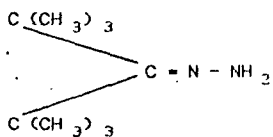
Institute of Chemistry, Łódź University,  
Narutowicza 68, 90 136 Łódź, POLAND

(Received 1 July 1988)

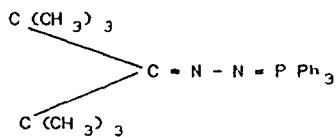
3-Hydrazo-2.2.4.4-tetramethylpentane and 3-triphenylphosphoranilideno-hydrazo-2.2.4.4-tetramethylpentane in acetonitrile and N.N-dimethylformamide by means of cyclic voltammetry on stationary solid electrodes (glassy carbon, Pt and Au) were studied. The catalytic effects of the nature and state of the electrode surface and the solvent were investigated. Mechanisms were suggested for the redox reactions that these compounds undergo cathodic reduction and anodic oxidation. The potentials of the respective processes the diffusion coefficients, the observed standard rate constants and the electrode transfer coefficients were determined.

*Introduction*

This work deals with the electrodic oxidation and reduction of 3-hydrazones of 2.2.4.4-tetramethylpentane:



I



II

I: 3-hydrazo-2.2.4.4-tetramethylpentane.

II: 3-triphenylphosphoranilidenohydrazo-2.2.4.4-tetramethylpentane.

The electrode reactions were carried out in acetonitrile (AN) and N,N-Dimethylformamide (DMF), with  $\text{Bu}_4\text{NClO}_4$  ( $10^{-1}$  mol. $\text{dm}^{-3}$ ) as a supporting electrolyte.

Compounds I and II were synthesized and examined some time [1-4]. The products of their chemical oxidation are the corresponding azines [5, 6].

The electrochemical reduction of the hydrazones was examined polarographically in acid and neutral aqueous solutions [7-9]. The oxidation of keto-arylhydrazones in water-AN solutions gives the appropriate ketones, while the oxidation of cyclic hydrazones such as 3.5.5-trimethyl-2-pyrazoline gives 3.3-dimethylbutan-2-one [10].

The electrooxidation of hydrazones on the platinum electrodes in non-aqueous AN was described by Barbey et al. [11] and Chiba et al [12]. Barbey oxidized 3-hydrazo-dibenzophenone voltammetrically, while Chiba oxidized its phenyl-substituted derivatives ( $x = -\text{H}$ ;  $-\text{CH}_3$ ;  $-\text{OCH}_3$ ;  $-\text{Cl}$ ) amperometrically.

In both cases, platinum electrode were used as working electrodes, and the almost identical experimental conditions ( $\text{LiClO}_4$  as a supporting electrolyte, concentration of hydrazones in mmol. $\text{dm}^{-3}$  range) permit acceptance of the suggestion [11, 12] as a basis for discussion in this work.

In both works the corresponding azines were obtained as final products, whereas there were different proposals concerning the mechanisms of the reaction, depending on the composition of the solution, the experimental conditions and the nature of the electrode.

### *Experimental*

Cyclic voltammetry (CVC) on compounds I and II was carried out by using the Wenking ST-72 apparatus and, the XY Houston Instruments 2000 recorder with IR<sub>e</sub> compensation.

The CVC measurements were conducted in the range of the sweep potential polarization rate from  $v = 0.010 \text{ V.s}^{-1}$  to  $v = 0.400 \text{ V.s}^{-1}$  in the classical thermostatic ( $298 \pm 0.5$ ) K and hermetic vessel of  $90 \text{ cm}^3$  volume made by METROHM.

The following working electrodes were used:

- A polished glassy carbon electrode (GCE) SIGRI with geometrical surface area  $A_1 = (0.44 \pm 0.02) \text{ cm}^2$ , put in the epoxide-glassy holder with the electric contact. Before each measurement, the electrode was polished with the diamond pastes of 30, 6, 3 and  $1 \mu\text{m}$  and  $\text{Al}_2\text{O}_3$  of  $0.05 \mu\text{m}$  and it was then rinsed with acetone, triple distilled water, and finally ether-dried. The GCE was then prepared electrochemically according to the literature [13-16].

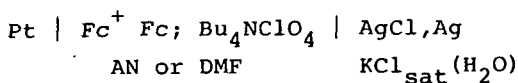
- A polished platinum electrode ( $\text{Pt}_{\text{pol}}$ ) with a geometrical area  $A_2 = (0.44 \pm 0.02) \text{ cm}^2$  prepared as the GCE.

- A polycrystalline gold electrode ( $\text{Au}_{\text{app}}$ ) with a geometrical area  $A_3 = (0.09 \pm 0.02) \text{ cm}^2$ . Golden wire with  $\phi = 0.15 \text{ cm}$  was put in a teflon holder after baths in concentrated  $\text{HNO}_3$  and in triple distilled water and was prepared for the

measurements by means of the sweep potential rate method, i.e. by cyclic polarization method, in the range from the hydrogen evolution potential to the oxygen evolution potential in an aqueous solution of  $\text{HClO}_4$  ( $5.10^{-1} \text{ mol.dm}^{-3}$ ).

After production of the "model" polarization curve [17, 18], the  $\text{Au}_{\text{app}}$  electrode was used for measurements. This method permitted reproducibility of measurements within  $\pm 0.5\%$  [19]. In relation to the surface of the polished electrode, the stabilized electrode  $\text{Au}_{\text{app}}$  has a surface development coefficient of  $4.0 \div 4.1$  [20]. In this way, the surface area  $\text{Au}_{\text{app}}$  is close to the surfaces of  $A_1$  and  $A_2$ .

The auxiliary electrodes were made of platinum mesh and were separated from the working part of the electrolyte by diaphragm of porous glass. In all measurements, the  $\text{AgCl/Ag}$  electrode in  $\text{KCl}_{\text{sat}}$  aqueous solution (METROHM) was used as a reference electrode in AN and DMF. All the potential values given in this work are referred to the reference electrode used. To allow a comparison of the measured potentials with the results obtained in the other solvents, additional measurements were carried out with reference to the "ferrocene potential scale" [21, 22] it is commonly used. The CVC loop ( $v = 0.100 \text{ V.s}^{-1}$ ) was registered in the following system:



The formal potential values:

$$E_f^{\text{O}} = 1/2 (E_{\text{p,a}} + E_{\text{p,c}}) \text{ were equal} \\ \text{DMF } E_f^{\text{O}} = (0.450 \pm 0.005) \text{ V vs ref. electrode,}$$

$$AN_{E_f}^O = (0.500 \pm 0.005) \text{ V vs ref. electrode,}$$

in accordance with the literature [23].

The examined compounds readily undergo hydrolysis or redox reactions in the presence of minute quantities of water or oxygen.

In the presence of water > 0.05 w %, the compound II is reduced irreversibly to phosphazine. Accordingly, the water was carefully removed from the supporting solutions with molecular sieve 4A and freezing-out in liquid nitrogen, and they were forced through to the measurement cell using argon. The glass ampoule with the examined compound was crushed in the cell where the overpressure of dry argon was kept. The outlet of argon was possible with the appropriate syringe.

Compounds I and II were examined at concentrations of  $4.2 \cdot 10^{-3}$ ,  $9.3 \cdot 10^{-3}$  and  $2.54 \cdot 10^{-2}$  mol.dm<sup>-3</sup>,  $1 \cdot 10^{-3}$  mol dm<sup>-3</sup> tetrabutylperchlorate (Bu<sub>4</sub>NClO<sub>4</sub>) was used as a supporting electrolyte. The measurements were conducted in the range of the sweep potential polarization rate from  $v = 0.02 \text{ V} \cdot \text{s}^{-1}$  to  $v = 0.200 \text{ v} \cdot \text{s}^{-1}$ .

Analysis of the CVC curves was carried out according to Nicholson and Shain [24, 25]. The function of irreversibility  $\psi = f(\Delta E_p)$  for calculating the observed rate constant ( $k_s$ ) was calculated from polynomial:

$$\Delta E_p = a \psi + b \psi^{-1} + c \psi^{-1/2} + \dots$$

where:  $a = 20.615$ ;  $b = -1.40167$ ;  $c = 3.4033 \text{ E-2}$ ;  
 $d = -3.37491 \text{ E-4}$ ;  $e = 3.79258 \text{ E-7}$ ;  $f = 1.74068$   
 $\text{E-8}$ ;  $g = -9.4157 \text{ E-11}$ ;  $h = -1.70248 \text{ E-13}$ ;  
 $i = 1.84194 \text{ E-15}$ ;  $j = 5.54909 \text{ E-19}$ .

The application of this equation gave results compatible with the calculation using Heinz's [26] suggestion for  $\Delta E_p = 80 \div \div 150$  mV within the limits of the mean square error of the average value.

### Results and discussion

The CVC curves of compound I on the stationary solid electrodes in AN are presented in Figs. 1-3. In the cathodic process hydrazone I is reduced irreversibly at a potential  $E_{p,c} = 0.5 \div -1.1$  V (depending on the type of the electrode) according to the scheme after [7-10]:

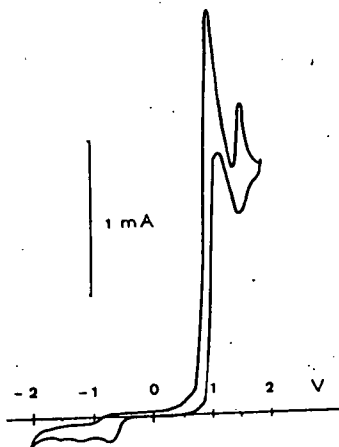
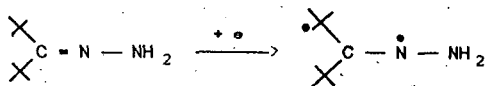


Figure 1.: Cyclic voltammogram of compound I in acetonitrile on glassy carbon electrode. Supporting electrolyte:  $1 \cdot 10^{-1}$  mol dm<sup>-3</sup> Bu<sub>4</sub>NClO<sub>4</sub>;  $C_I = 2.54 \cdot 10^{-2}$  mol dm<sup>-3</sup>;  $v = 0.100$  V s<sup>-1</sup>.



It has been pointed out that this reaction is independent of the anodic reactions that compound I undergoes. The electrochemical processes occur in the range of the  $+0.7 \div +1.8$  V polarization potentials.

For the electrooxidation of hydrazones, Chiba [12] proposes with the separation of nitrogen and the suggested of

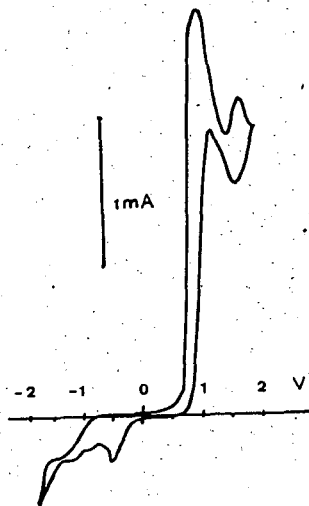
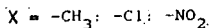
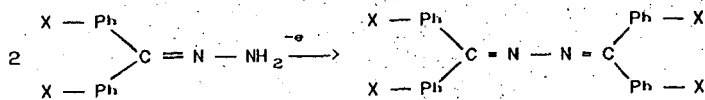
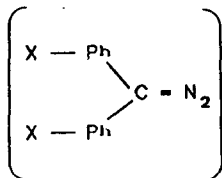


Figure 2.: Cyclic voltammogram of compound I in acetonitrile on polished platinum electrode; other parameters as in Fig. 1.



transitory formation:



The amperostatically performed electrooxidation proceeds in the potential range  $+0.7 \div +2.0 V_{sce}$ . The development of a potential of  $+2.0 V_{sce}$  by the working electrode was regarded [12].

As seen in Figs. 1-3, all the electrooxidation processes proceed in a similar range of potentials  $\pm 50 \text{ mV}$ , but their voltammetric characteristics are more precise.

Analysis of the CVC curves according to [24, 25] reveals the possibility of the following processes occurring in the range of the polarization potentials:

1. adsorption - desorption of substrates and reaction products;
2. the electrochemical reaction of electron transfer precedes the chemical reaction of dimerization;
3. the overall reaction is irreversible and its products are not reduced.

Similarly as in [12] the appearance of yellow crystals was observed. After purification in cool AN, they were identified (IR spectroscopy) as tetramethylpentane diazine.

Thus, the mechanism suggested by Barbey et al. [11] seems

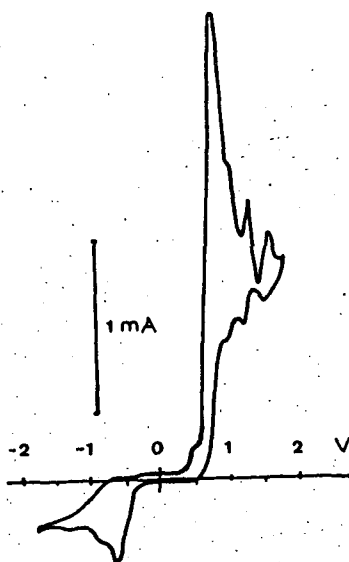
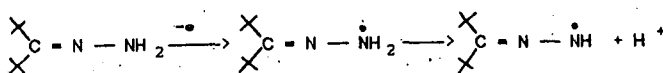
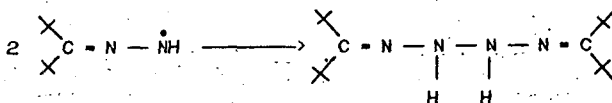


Figure 3.: Cyclic voltammogram of compound I in acetonitrile on the activated gold electrode. Other parameters as in Fig. 1.

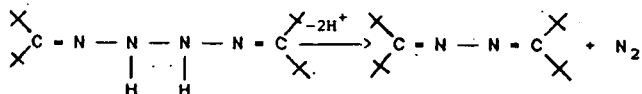
to be more probable:



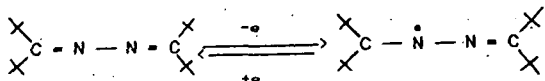
Then:



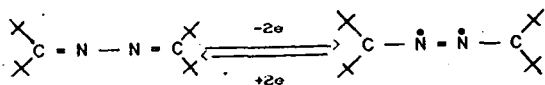
and finally:



Moreover, in the potentials interval  $+1.5 \div 1.8$  V in Figs 1-3. the loop probably relating to the reaction of electron transfer is visible:



or



In DMF the CVC curves on gold and platinum electrodes permit separation of the CVC loop (Fig. 4), suggesting the possibility of quasi-reversible reactions at potential  $E_f^0 = (-0.800 \pm 0.02)$  V:

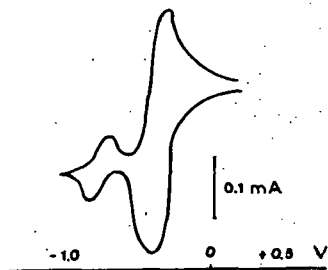
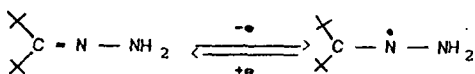


Figure 4.: Cyclic voltammogram of compound I in DMF on polished platinum electrode:  $c_I = 9.3 \cdot 10^{-3}$  mol·dm<sup>-3</sup>;  $v = 0.04$  Vs<sup>-1</sup>



with the parameters calculated for the polished platinum electrode:

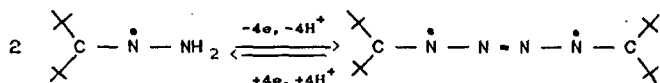
$$D_{\text{Ox}} = (1.1 \pm 0.04) \cdot 10^{-7} \text{ cm}^2 \text{ s}^{-1}$$

$$D_{\text{Red}} = (1.0 \pm 0.03) \cdot 10^{-7} \text{ cm}^2 \text{ s}^{-1}$$

$$\alpha n_{\alpha} = (0.064 \pm 0.04)$$

$$k_s = (1.24 \pm 0.11) \cdot 10^{-4} \text{ cm s}^{-1}$$

At potential  $E_f^0 = (-0.315 \pm 0.05) \text{ V}$  on  $\text{Pt}_{\text{pol}}$  we have:



with parameters:

$$D_{\text{Ox}} = (2.3 \pm 0.08) \cdot 10^{-7} \text{ cm}^2 \cdot \text{s}^{-1}$$

$$D_{\text{Red}} = (1.1 \pm 0.05) \cdot 10^{-7} \text{ cm}^2 \cdot \text{s}^{-1}$$

$$\alpha n_{\alpha} = (0.66 \pm 0.04)$$

$$k_s = (2.60 \pm 0.31) \cdot \text{cm} \cdot \text{s}^{-1}$$

At potentials  $> +0.7 \text{ V}$  the irreversible chemical reaction of formation of diazine proceeds. The current value for this reaction is constant in the range  $+0.7 \div +1.6 \text{ V}$ . and is independent of the sweep potential polarization rate. The presence of diazine was proved as in works [11, 12].

The electrodic processes of phosphoranilidenohydrazone II proceeded similarly to those of I. proving both the catalytic influence of the nature and the surface of the electrode and the influence of the solvent on the examined

process.

The influence of the solvent is visible both in the dependence on Gutmann's donor number  $^{AN}DN = 14.1$ ;  $^{DMF}DN = 27.0$ . and on the ability to create strong solvates (AN) or the nature of the interaction with compounds containing an active hydrogen atom (DMF).

Figure 5 exemplifies the CVC curve of a hydrazone. This CVC curve on a platinum electrode suggests a process close to the quasi-reversible reaction with a potential  $E_f^0 = (-0.25 \pm 0.01)$  V and the two-stage ( $E_{p,a} = +0.7$  V and  $E_{p,a} = +1.25$  V) irreversible electrochemical-chemical process.

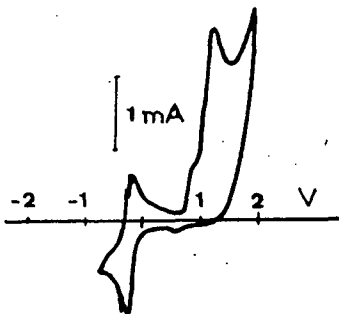


Figure 5.: Cyclic voltammogram of compound II in AN on the activated gold electrode;  $v = 0.100 \text{ Vs}^{-1}$ ;  $c_{II} = 2.54 \cdot 10^{-2} \text{ mol} \cdot \text{dm}^{-3}$

The process with a formal potential  $E_f^0 = -0.25$  V is a quasireversible reaction connected with the adsorption - desorption of substrates and reaction products. This was indicated by the additional small peaks visible below  $E_{p,c}$  on the cathodic branch and in front of the  $E_{p,a}$  peak on the

anodic branch of the CVC loop. Thus, Nicholson and Shain's model cannot be applied to calculate the parameters of this electrodic reaction.

Change of the solvent to DMF clearly revealed the influence both of the electrode material and of the nature of the solvent on the electrodic processes of compound II (Fig. 6).

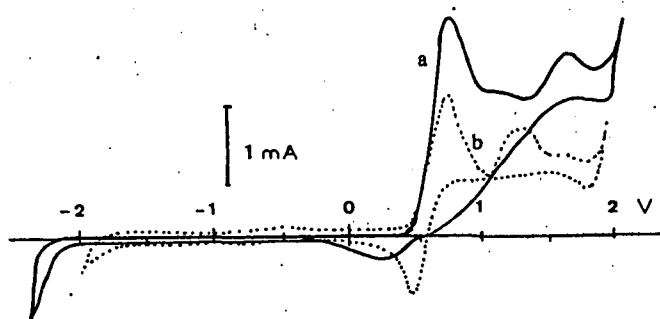


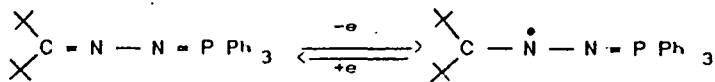
Figure 6.: Cyclic voltammogram of compound II in DMF on the glassy carbon electrode (a) on platinum (b); other parameters as in Fig. 5.

Complex anodic processes were studied both on the GCE electrode curve (a) and on the platinum electrode (b). Owing to the lack of the active group ( $=N-NH_2$ ), this hydrazone does not undergo reduction in the whole range of cathodic polarization.

On the plished platinum electrode, the separated CVC loop yielding the formal potential of the process.

$E_f^0 = (+0.610 \pm 0.02)$  V. fulfils the criteria of quasi-reversibility.

Thus, the following equation may be suggested for electrodic reaction:



with parameters:

$$D_{\text{Ox}} = (1.57 \pm 0.33) \cdot 10^{-7} \text{ cm}^2 \text{ s}^{-1},$$

$$D_{\text{Red}} = (1.88 \pm 0.35) \cdot 10^{-7} \text{ cm}^2 \text{ s}^{-1},$$

$$\alpha n_{\alpha} = (0.74 \pm 0.06)$$

$$k_s = (9.70 \pm 0.36) \cdot 10^{-5} \text{ cm} \cdot \text{s}^{-1}$$

The processes in the range of the potentials +1.1 ÷ + 1.8 V are independent of the sweep potential polarization rate.

#### Conclusions

1. The electrodic processes of 3-hydrazo-2.2.4.4-tetramethylpentane I and 3-triphenylphosphoranilidenohydrazo-2.2.4.4-tetramethylpentane II are dependent on the nature and the catalytic activity of the electrode and on the properties of the solvent.

2. The quasi-reversible electrodic processes of I and II on the platinum and gold electrodes in DMF allowed calculation of the basic parameters of the reaction: the diffusion coefficients  $D_{\text{Ox}}$  and  $D_{\text{Red}}$ , the electron transfer coefficient  $\alpha n_{\alpha}$  and the observed standard rate constant  $k_s$ .

3. The processes of anodic oxidation proceed according

to the suggested mechanism. As a result of anodic oxidation, I gives the corresponding diazine. It was not possible to separate the products of the anodic reaction of compound II.

#### *Acknowledgements*

The authors thank Prof. Günther Maier of the Institut für Organische Chemie, Giessen Universität, BRD, for providing compounds I and II and permitting certain measurements, and Prof. Mihály Novák of the Institute of Physical Chemistry, JATE University, Szeged, Hungary, for helpful discussions.

This work was supported by grant CPBP 01.15/4.08.

#### *References*

- [1] Szmant, H.H., C. Ginnis: *J. Am. Chem. Soc.*, 72, 2890 (1950).
- [2] Barton, D.R.H., F.S. Guziec jr, I. Shahak: *J. Chem. Soc. Perkin Trans. I.*, 1794 (1974).
- [3] Back, T.G., D.H.R. Barton, M.R. Britten-Kelly, F.S. Guziec jr: *J. Chem. Soc. Perkin Trans. I.*, 2079 (1977).
- [4] Röcker, E.: Thesis, Giessen Univ. (1980).
- [5] Barton, D.H.R., R.E. O'Brien, R. Steiner: *J. Chem. Soc.*, 470 (1962).
- [6] Elsert, B., M. Regitz, G. Heck, H. Schwall: *Methoden der Organische Chemie (Houben-Weyl)*, G. Thieme Verlag, Stuttgart 1968. vol. 10/4. p. 574.
- [7] Lund, H.: *Acta Chem. Scand.* 13, 249 (1959): *Discuss. Faraday Soc.*, 45, 193 (1968).



- [8] *Holleck, L., B. Kastening: Z. Elektrochem., 60, 127 (1956).*
- [9] *Baizer, M.M.: Organic Electrochemistry, Marcel Dekker, New York 1973.*
- [10] *Lin, E.-C., M.R.V. Mark: J. Chem. Soc. Commun., 1176 (1982).*
- [11] *Barbey G., J. Huguet, C. Caullet: Compt. Rend., 275C, 435, (1972).*
- [12] *Chiba, T., M. Okimoto, H. Nagai, Y. Takata: J. Org. Chem., 48, 2968 (1983)*
- [13] *Engstrom, R.C.: Anal. Chem., 54, 2310 (1982); ibid 56, 133 (1967).*
- [14] *Ravichandran, K., R.P. Baldwin: Anal. Chem., 57, 1744 (1984).*
- [15] *Thornton, D.C., K.T. Corby, V.A. Spendal, J. Jordan, A. Robba jr, D.J. Rustrom, M. Gross, G. Ritzler: Anal. Chem., 57, 150 (1985).*
- [16] *Halbert, M.K., R.-P. Baldwin: Anal Chem., 57, 591 (1985).*
- [17] *Ferro, C.M., A.J. Calandra, A.J. Arvia: J. Electroanal. Chem., 55, 291 (1974).*
- [18] *Angell, D.M., T. Dickinson: J. Electroanal. Chem., 35, 55 (1972).*
- [19] *Jakuszewski, B., H. Scholl: Polish J. Chem., 52, 1203 (1978).; ibid. 53, 1855 (1979).*
- [20] *Romanowski, S., H. Scholl: Elektrokhim., 16, 530 (1966).*
- [21] *Schneider, H., H. Strehlow: J. Electroanal. Chem., 12, 530 (1966).*
- [22] *Strehlow, H.: Electrode Potential in Non-Aqueous Solvents in Chemistry of Non-Aqueous Solvents ed. L. Lagowski, Acad. Press. New York 1967.*
- [23] *Bauer, D., M. Breant: in Electroanalytical Chemistry, ed. A.J. Bard. M. Dekker, New York, vol. 8 p. 281. (1975).*
- [24] *Nicholson, R., I. Shain: Anal. Chem., 36, 704 (1964); ibid. 36, 722 (1964); ibid. 37, 178 (1965).*
- [25] *Nicholson, R.: Anal. Chem., 37, 2310 (1967); ibid. 37, 135 (1967).*
- [26] *Heinze, J.: Ber. Bunsenges. Phys. Chem., 85, 1096 (1981).*

ЭЛЕКТРОДНЫЕ ПРОЦЕССЫ ПРОИЗВОДНЫХ 2,2,4,4-ТЕТРАМЕТИЛПЕНТАНА  
НА НЕПОДВИЖНЫХ ТВЕРДЫХ ЭЛЕКТРОДАХ. I. ЦИКЛИЧЕСКАЯ ВОЛЬТАМЕТ-  
РИЯ 3-ГИДРАЗОНОВ 2,2,4,4-ТЕТРАМЕТИЛПЕНТАНА

Х. Шолл и П. Кричмоник

Изучены методом циклической вольтометрии на неподвижных твердых электродах (Сс) ( $Pt_{пол}$ ) и ( $Au_{алл}$ ) 3-гидразо-2,2,4,4-тетраметилпентан и 3-трифенилфосфоранилидено-2,2,4,4-тетраметилпентан в ацетонитриле и в  $N,N'$ -диметилформамиде. Характеризованы каталитическое действие материала и состояния поверхности электрода, а также растворителя на протекающие процессы. Предложены механизмы окислительно-восстановительных реакций, происходящих при катодном восстановлении и анодном окислении изучаемых соединений. Определены значения потенциалов для соответствующих процессов, величины диффузионных коэффициентов и электронных передач. Определены также стандартные коэффициенты скоростей реакций.

ELECTRODIC PROCESSES OF 2,2,4,4 - TETRAMETHYLPENTANE  
DERIVATIVES ON STATIONARY SOLID ELECTRODES. II.  
VOLTAMMETRY OF 3,3'- DIBROMO - 2,2,4,4 - TETRAMETHYL -  
PENTANE IN DMF

By

H. SCHOLL AND P. KRZYCZMONIK

Institute of Chemistry, Łódź University  
Narutowicza 68, 90 136 Łódź, POLAND

*(Received 1 July 1988)*

The electrodic processes of geminal 3,3'-dibromo-2,2,4,4-tetramethyl pentane in DMF solution, with tetrabutylammonium perchlorate as supporting electrolyte, were examined by means of cyclic voltammetry and controlled potential electrolysis on glassy carbon, platinum and gold electrodes. The reaction products were examined by using HPLC, gas chromatography and <sup>1</sup>H NMR methods.

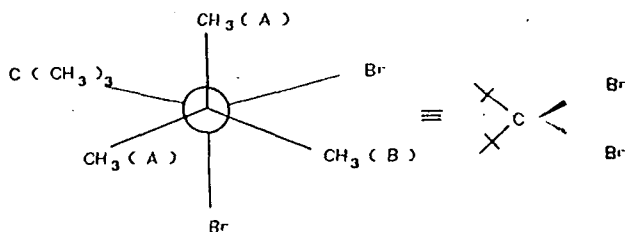
As a result of the electroreduction processes, monobromide and simple aliphatic compounds were obtained in two-stage processes with

$E_{p,c}^1 = -1.00$  V and  $E_{p,c}^2 = -2.00$  V vs AgCl (KCl<sub>sat</sub>, H<sub>2</sub>O), Ag reference electrode.

The complex processes of electrooxidation ( $E > +1.00$  V) probably lead to the formation of the radical cation BTMP<sup>•+</sup> and TMP<sup>++</sup>, which are strongly solvated in DMF or form ionpairs with the appropriate anions of the supporting electrolyte.

## Introduction

Geminal tetramethylpentane dibromide (DBTMP) was subjected to cyclic voltammetry experiments and controlled potential electrolysis. It is a white, crystal line compound with  $T_{mp} = 448 \text{ K}$ ,  $\delta^1\text{H NMR}$  (303 K, TMS,  $\text{CDCl}_3$ ) = 1.49 nm and  $\delta^{13}\text{C NMR}$  = 110.1 nm. Its synthesis was described by Maier and Kalinowski [1].



Scheme I

DBTMP is an aliphatic geminal dihalide, which are characterized by strong steric stresses. The  $\delta^{13}\text{C NMR}$  of geminally substituted carbon atom in halogen derivatives shows deviations ( $\delta_{exp} - \delta_{calc}$ ) that increase with increase of the substituent size. Halogen derivatives of this type are thought to be very good models to illustrate the influence of the  $\gamma$  effect caused by chlorine atoms [1-4].

In the series  $\text{I} \rightarrow \text{Br} \rightarrow \text{Cl}$ , the  $\gamma$  effect on the atom of the (B) *gauche* methyl group to two halogen atoms decreases in the given series (13.4  $\rightarrow$  3.7  $\rightarrow$  1.7 ppm). The effect on the carbon atoms of the (A) methyl groups in Scheme I changes in the same direction (6.0  $\rightarrow$  3.7  $\rightarrow$  3.5 ppm) [1].

Geminal dihalides were earlier examined polarographical-

ly [2-4]. In this work we study the electrodic processes of DBTMP on stationary solid electrodes in N.N-dimethylformamide (DMF). We used cyclic voltammetry (CVC) and controlled potential electrolysis (CPE), supplemented with high-pressure liquid chromatography (HPLC), gas chromatography (GC) and  $^1\text{H}$  NMR spectrometry.

### *Experimental*

CVC and CPE were carried out with the typical apparatus:  
 - a PG-30/1 potentiostat with an LSG programming generator (ASP UL. Poland) and an EMG 79 812 XY recorder (Hungary) for the measurements conducted in Lodz University;

- a Wenking ST-72 potentiostat with a VSG-72 programming generator and Houston Instruments-2000 XY recorder in University of Giessen.

In CVC the measurements were conducted in the range of sweep potential polarization rate from  $v = 0.010 \text{ Vs}^{-1}$  to  $v = 0.300 \text{ Vs}^{-1}$  in the hermetic, thermostatic ( $298 \pm 0.5$ ) K three-electrode vessel of  $90 \text{ cm}^3$  volume made by METROHM.

The following working electrodes was used:

- A polished carbon electrode (GCE) SIGRI with geometrical surface  $A_1 = (0.38 \pm 0.02) \text{ cm}^2$ , polished with diamond paste of 30, 6, 3 and  $1 \mu\text{m}$  and then with  $\text{Al}_2\text{O}_3$  of  $0.05 \mu\text{m}$  and prepared for the measurements according to the literature [5-8];
- a polished platinum electrode ( $\text{Pt}_{\text{pol}}$ ) with geometrical area  $A_2 = (0.38 \pm 0.02) \text{ cm}^2$ , prepared in the same way as the GCE;

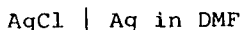
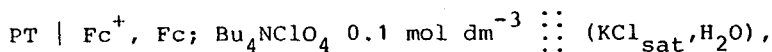
- a gold electrode ( $Au_{app}$ ) with geometrical area  $A_3 = (0.09 \pm 0.02 \text{ cm}^2)$ . prepared for the measurements by means of the "electrochemical sweep" method in an aqueous solution of  $HClO_4$  ( $0.5 \text{ mol dm}^{-3}$ ).

After production of the model polarization curve [9, 10] the reproducibility of the measurements was within the limits  $\pm 0.5 \%$  [11]. The stabilized surface of the gold electrode has the surface development coefficient 4.2 referred to the surface of the polished gold electrode [12]. In this way, the real surface of the  $Au_{app}$  is close to the surface areas  $A_1$  and  $A_2$ .

In the CPE method, a gold electrode ( $A_{4,geom} = 26 \text{ cm}^2$ ) and a platinum electrode ( $A_{5,geom} = 46 \text{ cm}^2$ ) were used, which were prepared for the measurements in the same way as  $Au_{app}$ .

In the measurements  $AgCl(KCl_{sat}, H_2O)$ ,  $Ag$ , METROHM was used as a reference electrode and the potential values given in this work refer to this electrode.

In order to permit comparison of the obtained potential values with the results obtained in other solvents, the CVC curve in the following system was registered:



This led to  $E_f^{DMF} = 0.450 \text{ V}$ , in accordance with literature [13].

Thus, the reference here is to the "ferrocene potential scale" [14, 15]. Although this is not regarded as perfect [16, 17], it is commonly used in the electrochemistry of non-aqueous solvents.

DBTMP readily undergoes hydrolysis. Accordingly, DMF was used after distillation according to the commonly used

methods [18];  $\text{Bu}_4\text{N}^+\text{ClO}_4^-$  dried in vacuum, served as supporting electrolyte. The solutions of the examined substance were kept for 48 hours over molecular sieve 4 Å. Then solutions were then forced through to the measurement cell by using dry argon. The concentrations of DBTMP for CVC were:  $8.7 \cdot 10^{-4}$ ,  $1.1 \cdot 10^{-3}$ ,  $3.3 \cdot 10^{-3}$ ,  $5.0 \cdot 10^{-3}$  and  $7.4 \cdot 10^{-3}$   $\text{mol} \cdot \text{dm}^{-3}$ , while for CPE  $1.25 \cdot 10^{-2}$   $\text{mol} \cdot \text{dm}^{-3}$  solution was used.

Analysis of the CVC curves was carried out according to Nicholson and Shain [19-21] and the electric charge used was determined by means of the CPE method from the dependence  $I = f(t)$ .

The products of the reaction was examined by HPLC with a Zeiss-PM-2 DL spectrometer and a Knauer refractometer with Spectra Physics instrumentation. After n-pentane extraction, the reaction products were further identified by GC with a Varian-aerograph-1400 with a Spectra Physics-autolag system I integrator. For  $^1\text{H}$  KMR spectrometry, a Varian T-60 was used.

### *Results and discussion*

The polarization potential ranges for the supporting electrolyte were: GCE: - 2.65 to +1.45 V;  $\text{Pt}_{\text{pol}}$ : -2.0 to +1.40 V;  $\text{Au}_{\text{app}}$ : -2.10 to +1.45 V; these data are in accordance with commonly known literature data. The capacity current in the supporting electrolyte was subtracted from the recorded currents of the electrodic processes.

A typical CVC curve for  $c_{\text{DBTMP}} = 3.3 \cdot 10^{-3}$   $\text{mol} \cdot \text{dm}^{-3}$  is given in Figure 1. It should be noted that, under conditions of our experiment, the adsorption of depolarizer molecules is possible. In the DBTMP molecule, the two bromine atoms are usually oriented towards the electrode surface, particularly

when it is positively charged; the influence of the *gauche* methyl group on the adsorption of the symmetrical bromine atoms is not known.

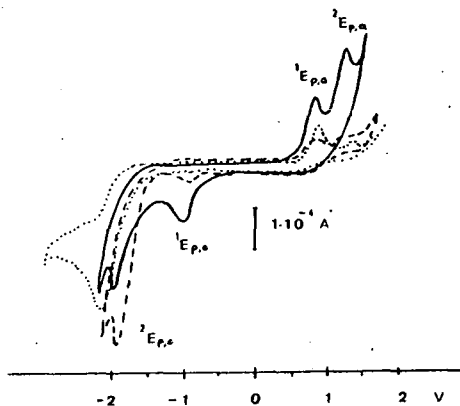


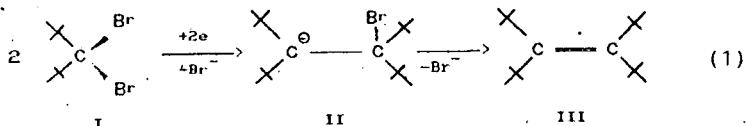
Figure 1.: Cyclic voltammograms DBTMP of  $c = 3.3 \cdot 10^{-3}$  mol dm<sup>-3</sup>; reference electrode AgCl (KCl<sub>sat</sub> H<sub>2</sub>O), Ag; supporting electrolyte Bu<sub>4</sub>N<sup>+</sup>ClO<sub>4</sub><sup>-</sup> (0.1 mol dm<sup>-3</sup>)  $v = 0.1$  Vs<sup>-1</sup>; in DMF. GCE: ... Pt<sub>pol</sub>: - - - - ; Au<sub>app</sub>: — .

With selected ranges of the polarization potentials, the electroreduction and electrooxidation processes were found to be independent of one another and the of the nature of the electrode.

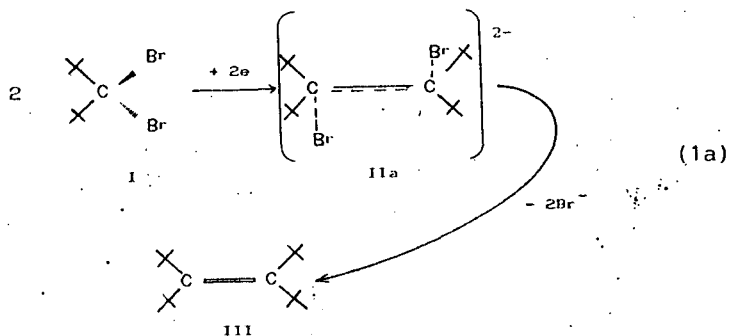


(i) *Electroreduction processes*

The most desirable product of the electroreduction of DBTMP would be tetra-tert-butylethylene, sought in both chemical [22] and electrochemical [2] processes. The mechanism of such a reaction could be as in equations (1) and (1a):

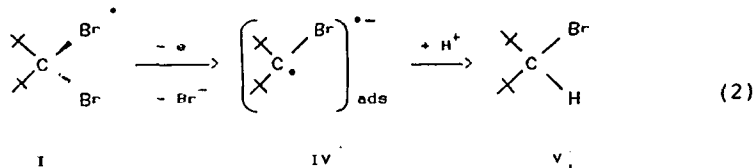


OR:



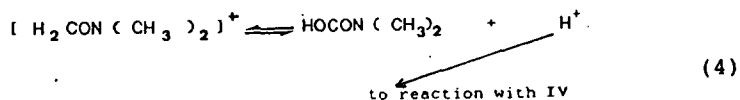
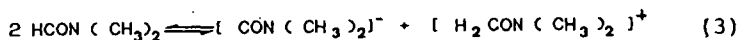
Our experiment revealed another mechanism of the electroreduction process. On the GCE electrode (Fig. 1), a single-stage process of reduction at the potential  ${}^2E_{p,c} = -1.95$  to  $-2.00$  V is visible. On the Pt<sub>pol</sub> electrode, a small peak with  ${}^1E_{p,c} = -0.95$  to  $-1.00$  V appears. At the same potential values on the Au<sub>app</sub> electrode peak currents  ${}^1I_{p,c} \approx {}^2I_{p,c}$ , clearly indicating the two-stage process of DBTMP electroreduction.

Electrolysis at a potential  ${}^1E_{p,c} = -0.95$  V leads to the formation of 2,2,4,4-tetramethylpentane monobromine according to Equation (2):



This result, which differs from expectations, may be explained as follows:

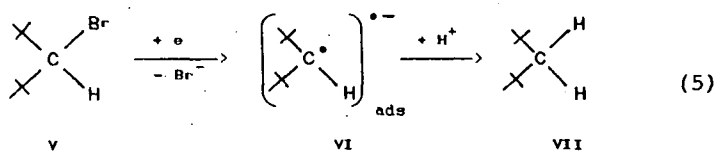
1. The sterically differentiated methyl groups (A and B) cause the adsorption of Br oriented towards the electrode. It may be assumed that the *gauche* methyl group B has a decisive influence on this process.
2. According to the known electrode properties, activated Pt and Au electrodes catalyse the process of electroreduction of Br with the formation of anion radical IV (Equation 2).
3. Anion radical IV generated on the electrode is a strong base, which acquires a proton after shift of the autodissociation equilibrium of DMF [23]:



After the flow of equivalent charge  $\approx 1 \text{ F} \cdot \text{mol}^{-1}$ , peaks a and b (Fig. 2) are of similar heights.

Additional confirmation of the suggested mechanism of the reaction may be negative result of the analogous attempt

in acetonitrile.



In the next stage of electroreduction, at the potential  ${}^2E_{p,c} = -2.00$  V monobromide v is reduced to 2,2,4,4-tetramethylpentane.

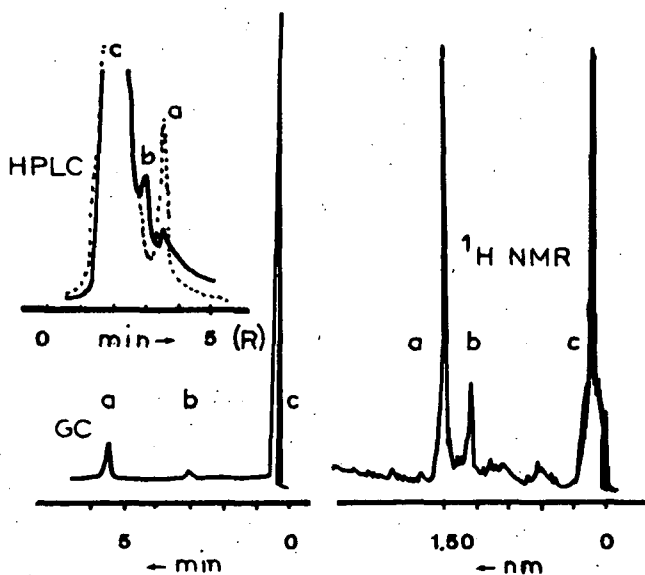


Figure 2.: Spectral analysis of products of electroreduction reactions: a - 3,3'-dibromo-2,2,4,4-tetramethylpentane; b - 3-bromo-2,2,4,4-tetramethylpentane; c - DMF and supporting electrolyte.

Peak a (Fig. 2) vanishes in favour peak b after the flow of the equivalent charge  $2 F \cdot \text{mol}^{-1}$ . Thus the mechanism of the second stage of the electroreduction may be suggested to be as in equation (5).

(ii) *Electrooxidation processes*

In the anodic branch of the polarization curve, the electrooxidation of DBTMP also exhibits two stages (Fig.1). The processes are characterized by the following peak currents: a clearly flattened peak with potential

$${}^1E_{p,a} = +0.90 \text{ to } +1.10 \text{ V, and a sharp peak with potential } {}^2E_{p,a} = +1.35 \text{ V.}$$

Similarly as in the above-described examinations of the electroreduction processes, CPE was conducted at  ${}^1E_{p,a}$  and  ${}^2E_{p,a}$ .

The charges used were 1.22 and  $0.82 F \text{ mol}^{-1}$ . The HPLC, GC and  ${}^1\text{H}$  NMR analysis demonstrated the loss of peaks a (Fig. 2) without the appearance of new spectra characteristic of other linking. Thus, it may be assumed that strongly ionized products are formed in the solution, whose spectra are similar to those of the solvent and supporting electrolyte (peaks c in Fig.2).

Extraction attempts with a typical non-polar solvent (n-pentane) did not reveal the reaction products in the liquid phase. It is obvious that, after the addition of water to precipitate  $\text{Bu}_4\text{N}^+\text{ClO}_4^-$ , the hydrolysis always led to 2.2.4.4-tetramethylpentanol.

Examinations of the compounds of the type tetra-tert-butyl-tetrahydrene [24, 25] have shown electron transfer is hindered by steric barriers, and ion radicals may be formed under the conditions of anodic oxidation. This was concluded because cation radicals observed with ESR methods were

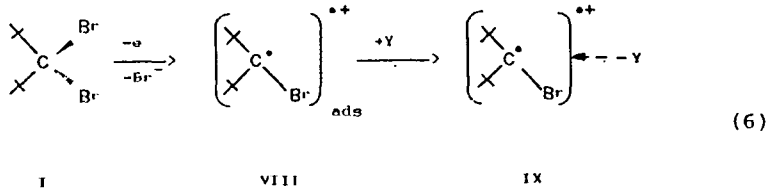
identical with the cation radicals generated by means of classical chemical oxidation. Those reactions are catalysed under the appropriate Lewis' acid-base conditions, and the products are captured in the special "traps". In this case, the parallel observations by means of spectral methods (e.g. *in situ* CVC-ESR) or freezing of the reaction products were used. These methods were also used in the work of Fox et al. [24]. The information that CVC was performed at 203 K in their work does not seem to be very reliable, because of the melting point of acetonitrile (232 K).

The CVC curves recorded at 253 K are more reliable [25]. In this way, many cation radicals of type  $R^{\cdot+}$  were isolated from the group of tetra-tert-butyl compounds. Their structures were determined by using MNDO-UMF or MNDO-RHF methods [25, 26].

Thus, the process carried out by means of CVC methods even at the sweep potential polarization rate to  $10 \text{ Vs}^{-1}$  in the oscilloscopic observation of curves and CPE at 298 K is an extremely fast reaction. The transformation to other forms of the generated compounds is also possible. Such reasoning is to be found in the earlier work of Miller [26] where, for a similar group of compounds on a platinum electrode at 0.6 V, a signal impossible to interpretation was obtained.

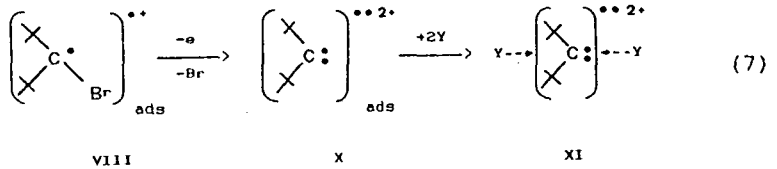
Thus, since the products of DBTMP electrooxidation give spectra in the same range as the "background", the mechanism of the anodic oxidation of DBTMP may be suggested only as probable. To a first approximation, the mechanism of the electrochemical processes taking place at a potential

$^1E_{p,a} = +0.90 \text{ V}$  is:

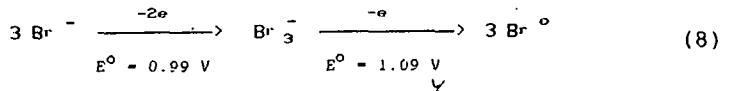


where  $Y = \text{DMF}$  or  $\text{ClO}_4^-$

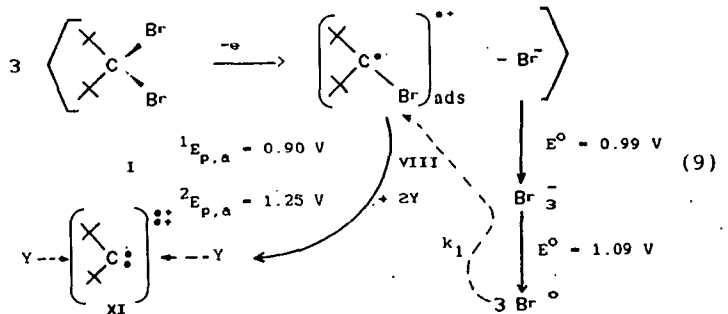
and then at a potential  $^2E_{p,a} = +1.35 \text{ V}$ :



The broad peak at  $^1E_{p,a}$  and the literature data [13] indicate the possibility of the existence of the parallel process in the potential range  $^1E_{p,a}$  to  $^2E_{p,a} = +0.90$  to  $+1.35 \text{ V}$ . This process involves the oxidation of  $\text{Br}^-$  ion and the consequent appearance of a new chemical oxidizer [13]:



The existence of such a process was proved by analysis of Nicholson and Shain [19, 20]. On this basis, the mechanism of the anodic oxidation of DBTMP suggested in Equations (6) and (7) is as follows:



The cation radicals of type XI formed are solvated in the reaction environment or they form ionpairs with the anions of the supporting electrolyte.

### *Conclusions*

The preparative processes of controlled potential electrolysis do not promise great success in this group of sterically stressed geminal compounds. On the other hand, the use of generated radicals of types VII and XI as mediators of the chemical oxidation of the other organic compounds in homogeneous emulsions seems to be very interesting.

### *Acknowledgements*

The authors are grateful to Prof. G. Maier and Dr. E. Röcker of the Institut für Organische Chemie, Justus Liebig Universität Giesse (BRD), for providing DBTMP and making possible certain experimental examinations. We thank Prof. Mihály Novák of the Institute of Physical Chemistry, JATE University, Szeged, for helpful discussions.

The investigation was conducted with the partial support of grant CPBP 01.15/4.08

## References

- [1] Kalinowski, H.O., E. Röcker, G. Maier: *Org. Magn. Res.*, 21, 64 (1983).
- [2] Fry, A.J.: in *Synthetic Organic Electrochemistry*, Wesley, Univ. Harper and Row Publ. (1972) pp. 178-187.
- [3] Ayer, W.A., L.M. Brown, S.Fung, J.B. Stothers: *Can. J. Chem.*, 54, 3272 (1976); *Org. Magn. Res.*, 1, 73 (1978).
- [4] Eliel, E.L., W.F. Bailey, L.D. Kopp, R.L. Willer, D.M. Grant, R. Bertrand, K.A. Christiansen, D.K. Dalling, M.W. Duch, E. Wenkert, F.M. Schell, D.W. Cochran: *J. Am. Chem. Soc.*, 97, 322 (1975).
- [5] Engstrom, R.C.: *Anal. Chem.*, 54 2310 (1982); *ibid.* 56, 136 (1984).
- [6] Thorton, D.C., K.T. Corby, V.A. Spendel, J. Jordan, A. Robbat jr, D.J. Rustrom, M. Gross, G. Ritzler: *Anal. Chem.*, 57, 591 (1985).
- [7] Ravichandran, K., R.P. Baldwin: *Anal. Chem.*, 57, 1744 (1984).
- [8] Halbert, M.K., R.P. Baldwin: *Anal. Chem.*, 58, 591 (1985).
- [9] Ferro, C.M., A.J. Calandra, A.J. Arvia: *J. Electroanal. Chem.*, 55, 291 (1974).
- [10] Angell, D.M., T. Dickinson: *J. Electroanal. Chem.*, 35, 55 (1972).
- [11] Jakuszevski, B., H. Scholl: *Polish. J. Chem.*, 52, 1203 (1978); *ibid.* 53, 1855 (1979).
- [12] Romanowski, S., H. Scholl: *Elektrochim.*, 16, 1184 (1980).
- [13] Bauer, D., M. Breant: in *Electroanalytical Chemistry*, ed. A.J. Bard, M. Dekker, New York (1975) vol. 8 p. 281.
- [14] Schneider, H., H. Strehlow: *J. Electroanal. Chem.*, 12, 530 (1966).
- [15] Strehlow H.: *Electrode Potential in Non-Aqueous Solvents in Chemistry of Non-Aqueous Solvents*, ed. L. Lagowski, Acad Press, New York (1967)
- [16] Parker, A.J.: *Chem. Revs.*, 69, 1, (1969).
- [17] Marcus, Y.: *Pure & Appl. Chem.*, 55, 977 (1983).
- [18] Baizer, M.M.: *Organic Electrochemistry*, M. Dekker, New York (1972).



- [19] *Nicholson, R., I. Shain: Anal. Chem., 36, 704 (1964);  
ibid. 36, 722 (1964); ibid. 37, 178 (1965).*
- [20] *Nicholson, R.: Anal. Chem., 37, 667 (1967); ibid. 37,  
135 (1967).*
- [21] *Olmstead, M., R. Nicholson: J. Electroanal. Chem., 14,  
133 (1967).*
- [22] *Buter, J., R.M. Kellog: J. Org. Chem., 42, 973 (1977).*
- [23] *Shahparonov, M.I., B. Raike, L.U. Lanshina: Fizika i  
Fizikokhimiya Zhidkosti. Khimia, Moskva (1973).*
- [24] *Fox, A.M., K.A. Campbell, S. Honig, H. Berneth,  
G. Maier, K.-A. Schneider. K.-D. Malsch: J. Org. Chem.,  
47, 3408 (1982).*
- [25] *Fox, M.A., K. Campbell, G. Maier, L.H. Franz: J. Org. Chem.,  
48, 1762 (1983).*
- [26] *Miller L.L., G.D. Norblom, E.A. Mayeda: J. Org. Chem.,  
37, 916 (1972).*

ЭЛЕКТРОДНЫЕ ПРОЦЕССЫ ПРОИЗВОДНЫХ 2,2,4,4-ТЕТРАМЕТИЛПЕНТАНА  
НА НЕПОДВИЖНЫХ ТВЕРДЫХ ЭЛЕКТРОДАХ. II. ВОЛЬТОМЕТРИЯ 3,3-  
ДИБРОМО-2,2,4,4-ТЕТРАМЕТИЛПЕНТАНА В ДИМЕТИЛФОРМАМИДЕ.

Х. Шолл, и П. Кричмоник

Изучены электродные процессы геминально замещенных 3,3'-дибромо-2,2,4,4-тетраметилпентана в ДМФ с  $0.1$  мол  $\text{дм}^{-3}$  концентрацией  $\text{Bu}_4\text{N}^+\text{ClO}_4^-$  в качестве электролита-носителя, путем циклической вольтометрии (свс) и электролиза с регулируемым потенциалом (срп) на электродах из стеклянного угля (сг), платины и золота. Продукты реакции контролировались методами жидкостной хроматографии высокого давления (нрлс), газо-жидкостной хроматографии (сг) и ядерного парамагнитного резонанса (1н-нмр).

В результате двухстадийных процессов электродного восстановления  $^1E_{p,c} = -1.00$  в и  $^2E_{p,c} = -2.00$  в  $\text{AgCl}(\text{KCl}_{\text{sat}}, \text{H}_2\text{O})\text{Ag}$ , образовались соответственно монобромид и алифатические соединения.

Сложные процессы электроокислации ( $E > +1.00\text{в}$ ), вероятно ведут к образованию катион-радикалов  $\text{BTMP}^+$  и  $\text{TMP}^{2+}$  сильно сольватированных в ДМФ, или образующих ионные пары с соответствующими анионами электролита-носителя.

STABILITY OF TiO<sub>2</sub> DISPERSIONS AT DIFFERENT pH VALUES  
AND IN PRESENCE OF AlCl<sub>3</sub> ELECTROLYTE

By

A.A. ADB EL HAKIM\*, E. TOMBÁČZ\*\* AND F. SZÁNTÓ\*\*

\* Lab. Polymers and Pigments, National Research Center,  
Dokki-Cairo, Egypt

\*\* Department of Colloid Chemistry József Attila University  
Szeged, Hungary

*(Received 15 June 1988)*

The stabilities of three different rutile (Bayer) samples, denoted RKB-2, Ru-2 and RSM-2, were investigated in aqueous medium. It was found that the RKB-2 sample was unstable between pH 5 and 9.5, Ru-2 was unstable at pH < 5, and RSM-2 was stable between pH 5 and 9. The effect of AlCl<sub>3</sub> electrolyte on the stabilities of these pigments was also studied. It was found that the RKB-2 sample lost its stability at electrolyte concentrations higher than 10 mmol dm<sup>-3</sup>, Ru-2 was unstable at any electrolyte concentration, and RSM-2 was stable at all electrolyte concentrations used.

*Introduction*

The behaviour of aqueous colloidal dispersions of metal oxides such as titanium dioxide is important in connection with industrial coatings and is an interesting field of colloid science. The existence of hydroxyl groups on the surface of titanium dioxide has been substantiated. In principle, these arise from the interaction of water vapour with the surface planes. The comprehensive experiments of Boehm [1] demonstrated the amphoteric nature of the titanium dioxide surface. There are two types of OH groups: one type is bound to one  $Ti^{4+}$  site (terminal), and the other type to two such sites (bridged OH). These would be expected to exhibit different chemical behaviour. Boehm suggested that the bridged groups should be strongly polarized by the cations and therefore they are acidic in character, while the terminal OH could be predominantly basic and exchangeable with other anions. Levine and Smith [2] found that in aqueous medium the isoelectric point (iep) is equal to the point of zero charge (pzc) when there is no specific adsorption in the inner region of the electric double layer. When adsorption occurs at the titanium dioxide/solution interface, the pzc and iep move in opposite directions as the concentration of the supporting electrolyte is increased. There is also a difference between the hydrous and dehydrated oxides as concerns the pzc values determined by Johanson and Buchanan [3].

In practice, there are two types of titanium dioxide, anatase and rutile. The main difference between them, as indicated by the energy of conversion of anatase into rutile, is that rutile has less ionic character [4]. When anatase is

heated to 800 °C, its surface charge changes in sign from positive to negative, which is ascribed to the change from anatase to rutile [5,6]. All OH groups on rutile have been shown to be reasonably strongly acidic, in contrast to the anatase surface [1].

The DLVO theory can be applied to a description of the stability of titanium dioxide dispersions in aqueous medium [1-6]. The coagulation behaviour of this oxide may be examined in terms of the electrokinetic or  $\zeta$ -potential, or by observation of coagulation series.

Furlong and Parfitt [7] studied the effects of surface crystallinity, dehydration and specific adsorption of anions and cations on the electrokinetic behaviour of titanium dioxide. They found that not only these factors affected the electrokinetic behaviour, but also the pretreatment of the oxide (e.g. heating, washing) before the dispersing process.

In the work of Wiese and Healy [8-11], it was found that the finite solubility of some oxides causes modification of the dissimilar surfaces. This then leads to a great difference in the rheology and stability of the suspensions.

The main purpose of our study was to investigate the stability of some rutile samples, depending on pH and  $\text{AlCl}_3$  electrolyte concentration.

#### *Materials and Methods*

Rutile titanium dioxide pigments denoted Ru-2, RKB-2 and RSM-2 were prepared by Bayer in commercial grade. The BET specific areas of the samples, determined by  $\text{N}_2$  adsorption, were 7.8, 10.4 and 5.9  $\text{m}^2/\text{g}$ , respectively. The chemical analysis data on the RKB-2 sample are given in Table I.

Table I

*Chemical analysis of RKB-2 TiO<sub>2</sub>*

Oxide	SiO <sub>2</sub>	Al <sub>2</sub> O <sub>3</sub>	TiO <sub>2</sub>	ZnO	Ignition loss
	%	%	%	%	%
Particle composition	2.8	2.2	93.5	0.04	1.6
Surface composition	16.6	47.1	36.4	-	

All chemicals used were of AR grade. Aluminium chloride was a product of Reachin (USSR). Potassium hydroxide and calcium chloride were from Reanal (Hungary). Lanthanum chloride was a Merck product.

The sedimentation measurements on titanium dioxide dispersions in aqueous medium (5 g/dm<sup>3</sup>) were carried out in a series of test tubes. The pH of dispersions was adjusted from 2 to 11, using dilute KOH or HNO<sub>3</sub>. Dispersions with different electrolyte concentrations up to 50 mmol AlCl<sub>3</sub>/dm<sup>3</sup> were made by dilution.

*Results**Effect of pH*

The stabilities of different types of titanium dioxide were studied at different pH values. The features of the sedimentation and the shaking number required to redisperse

the settled dispersion were determined. The results observed are given in Table II.

Table II

Effect of pH on stability of different  $TiO_2$  dispersicns

pH	RKB-2		RU-2		RSM-2	
	feature of settling	number of shakings	feature of settling	number of shakings	feature of settling	number of shakings
2	diffuse	44	sharp boundary	2	sharp boundary	2
3		70		2		2
4		28		2		2
5		12		2		26
6	sharp	10	diffuse	90	diffuse	37
7	boundary	5		180		41
8		13		50		30
9		17		58		26
10	diffuse	24	diffuse	50	sharp	17
11		116		66	boundary	18

It may be seen that the dispersions of RKB-2  $TiO_2$  are stable in highly acidic and basic media, but they lose their stability between pH 5.0 and 9.5. Wiese and Healy [8] found that dispersions of  $TiO_2$  are unstable only at pH values between 5.5 and 7.0. The difference between our results and those obtained by others [8] may be due to the fact that the surface of the  $TiO_2$  particles is modified, and for this reason it is heterogeneous. It is seen from Table I that the surface of  $TiO_2$  particles is formed mainly from  $Al_2O_3$  and  $TiO_2$  but the presence of  $SiO_2$  on the surface is not negligible.

The stability region is wide, which may be attributed to the existence of AlOH, SiOH and TiOH amphoteric sites on the surface of this sample.

The pzc values for the different oxides [15] are as follows:

	pzc
$\gamma\text{-Al}_2\text{O}_3$	9.1
$\alpha\text{-Al}_2\text{O}_3$	8.5
$\text{TiO}_2$	6.0
$\text{SiO}_2$	3.0

The charge of the amphoteric surface is positive at a pH lower than the pzc, and negative at a pH higher than the pzc. From examinations of the charge of each site which can exist on the surface of this  $\text{TiO}_2$  sample in different pH ranges, it is found that the situation is as follows:

pH range	sign of charge		
	<u>AlOH</u>	<u>TiOH</u>	<u>SiOH</u>
< 3	+	+	+
3...6	+	+	-
6...9	+	-	-
> 9	-	-	-

It can be seen that both positive and negative charges exist on the surface of the particles between pH 5 and 9. Heterocoagulation between surface parts of opposite charge takes place in this pH range. The suspensions become unstable and settle with a sharp boundary. The results on the stability region were confirmed by the shaking number required to redisperse the sediment. Table II shows that



this number is high at  $\text{pH} < 5$  and higher at  $\text{pH} > 9$ , indicating the formation of caked sediments which can only form from stabilized particles. The stability behaviour is correlated with the number of shakings: the larger this number, the more stable the dispersion.

The Ru-2  $\text{TiO}_2$  suspensions were stable at  $\text{pH} \geq 6$ , as can be seen in Table II, but they were unstable in acidic medium. The same results were obtained from the number of shakings for redispersion, which was small in acidic medium and large at  $\text{pH} \geq 6$ .

The third  $\text{TiO}_2$  sample (RSM-2) was found to be unstable in highly acidic and basic media, but it is stable for a short time at  $\text{pH} 5-9$ . This agrees with the shaking number results. The shaking number was found to be very small at  $\text{pH} < 5$ , somewhat higher at  $\text{pH} > 9$ , and large in the  $\text{pH}$  range 5-9.

These last two types of  $\text{TiO}_2$  differ in behaviour from the first. An explanation of their behaviour is not possible, because the surface modification is unknown.

#### *Effect of aluminium chloride*

The stabilities of  $\text{TiO}_2$  dispersions were studied in the presence of electrolyte. The results are shown in Table III.

The RKB-2  $\text{TiO}_2$  dispersion was unstable in aqueous medium, and the presence of a small amount of electrolyte (up to  $1 \text{ mmol dm}^{-3}$ ) had no effect. The  $\text{pH}$  of the dispersion was in the instability region given in Table II. The larger the electrolyte amount added, the more stable the dispersion in the concentration region  $2.5-5 \text{ mmol dm}^{-3}$ , where the  $\text{pH}$  was in the stable region given in Table II. The dispersion was increasingly unstable with increase of the electrolyte

Table III

Effect of electrolyte on stability of  $TiO_2$  dispersions

$AlCl_3$ mmol $dm^{-3}$	RKB-2		Ru-2		RSM-2				
	stability	no.of shakings	pH	stability	no.of shakings	pH	stability	no.of shakings	pH
-	unstable	5	7.0		3	6.6		19	6.9
1		19	5.1		32	3.3		20	5.0
2	stable	72	4.0		32	2.8		400	4.8
5		44	3.9		32	2.7		220	4.2
10	unstable	90	3.7	unstable	30	2.7	stable	98	4.1
15		85	3.5		30	2.6		24	4.0
20		92	3.1		20	2.4		20	3.9
50		100	2.9		20	2.2		20	3.8

concentration. This may be due to the coagulating effect of larger amounts of electrolyte.

The behaviour of the second sample (Ru-2) differed from that of the first one. It was unstable at all electrolyte concentrations. The pH of all dispersions was in the unstable pH region in Table II. This is also evident from the small number of shakings.

The last type of  $\text{TiO}_2$  dispersion, which was made from the RSM-2 sample, was stable in the presence of all amounts of electrolyte added. The pH-s of the dispersion, 6.9-3.8, were roughly in the stability region in Table II. This may be due to the complex-forming effect of  $\text{Al}^{3+}$  ions. The abnormal behaviour of aluminium salts has likewise been reported by others [12-14].

#### References

- [1] Boehm, H.P.: Discuss. Faraday Soc., 52, 264 (1971).
- [2] Levine, S. and A.L. Smith: Discuss. Faraday Soc. 52, 290 (1971).
- [3] Johanson, P.G. and A.S. Buchanan: Aust. J. Chem. 10, 398 (1957).
- [4] Bobyrenko, Yu. Ya., A.B. Zholnin and V.K. Konvalova: Russ. J. Phys. Chem. 46, 749 (1972).
- [5] Morimoto, T. and M. Sakamoto: Bull. Chem. Soc. Japan 37, 719 (1964).
- [6] Onishi, Y. and T. Hamamura: Bull. Chem. Soc. Japan 43, 996 (1970).
- [7] Furlong, D.N. and G.D. Parfitt: J. Colloid Interface Sci. 65, 548, (1978).
- [8] Wiese, G.R. and T.W. Healy: J. Colloid Interface Sci. 51, 427 (1975).
- [9] Wiese, G.R. and T.W. Healy: J. Colloid Interface Sci. 51, 434 (1975).

- [10] *Wiese, G.R. and T.W. Healy*: J. Colloid Interface Sci. 52, 452 (1975).
- [11] *Wiese, G.R. and T.W. Healy*: J. Colloid Interface Sci. 52, 458 (1975).
- [12] *Force, C.G. and E. Matijevic*: Kolloid Z. u. Z. Polymere 225, 33 (1968).
- [13] *Force, C.G. and E. Matijevic*: Kolloid Z.u.Z. Polymere 224, 51 (1968).
- [14] *Matijevic, E., G.E. Danauer and M. Kerker*: J. Colloid Interface Sci. 19, 333 (1964).
- [15] *James, R.O. and G.A. Parks*: in Surface and Colloid Science, Vol. 12. (Ed. Matijevic, E.) Ch. 2., Plenum, New York (1982).

СТАБИЛЬНОСТЬ ДИСПЕРСИЙ  $\text{TiO}_2$  ПРИ РАЗНЫХ pH СРЕДЫ И В ПРИСУТСТВИИ ЭЛЕКТРОЛИТА  $\text{AlCl}_3$

А. А. Абд Эл Хаким, Э Томбац и Ф. Санто

Изучена стабильность дисперсии трех различных образцов рутила (фирмы Bayer, РКВ-2, ru-2 и RSM-2) в водной среде. Было найдено, что дисперсии образцов РКВ-2 неустойчива в интервале pH среды от 5 до 9.5, ru-2 неустойчива при pH 5, а RSM-2 стабильна между pH 5 и 9. Найдено, что дисперсия образца РКВ-2 теряет свою стабильность при концентрациях  $\text{AlCl}_3$  превышающих  $10 \text{ ммоль/см}^3$ , дисперсия образца ru-2 нестабильна при любой концентрации электролита, а дисперсия образца RSM-2 стабильна при любых концентрациях  $\text{AlCl}_3$ .

EFFECT OF ELECTROLYTE CONCENTRATION ON STABILITY  
OF POLYMER LATEX

By

A. ABD EL HAKIM\*, E. TOMBÁ CZ\*\*, F. SZÁNTÓ\*\*

\* Lab. Polymers and Pigments, National Research Center,  
Dokki-Cairo, Egypt

\*\* Department of Colloid Chemistry, József Attila University,  
Szeged, Hungary

(Received 15 June 1988)

The surface charge of Litex BL 112 polymer latex (Hüls AG) was characterized by means of potentiometric and conductometric titrations. It was found that there are two types of acidic groups: a small amount of strongly acidic groups and a larger amount of weakly acidic ones, with a surface charge density of  $3.6 \mu\text{C}/\text{cm}^2$ . The acidic dissociation constant was found to be 4.2. The ccc-s of  $\text{CaCl}_2$ ,  $\text{AlCl}_3$  and  $\text{LaCl}_3$  were determined, and were found to be 34, 15.8 and  $2 \text{ mmol dm}^{-3}$ , respectively.

*Introduction*

The behaviour of dispersions of pigments and/or polymer latexes in an aqueous medium is important for paint technology and research. The interactions between polymer latex particles can be attributed to electric double-layer repulsion and van

der Waals attraction, both based on electric interactions [1]; these two types of interaction can be described on the basis of the DLVO theory. The van der Waals attractive forces decrease quickly with the distance between two particles. As the particles approach each other, the repulsive coulombic forces increase. The higher the charge density on the particles, the stronger the resulting repulsion between them, and therefore the existence of charges on the surface plays a determining role in the stability of a polymer latex. This theory is accepted by most scientists, but it was originally developed for the interactions between infinite flat plates or two spheres of equal sizes.

Hogg, Healy and Fuerstenau [2] extended the DLVO theory to the interactions of dissimilar spherical particles, i.e. for the case of heterocoagulation. The major parameters of the theory are the double layer potential of each type of particle, the ionic strength of the medium, the particle size, and the relative concentrations.

In the work of Ottewill et al [3-5], we find the characterization of a number of monodisperse systems, the polystyrene latex particles produced by the emulsion polymerization of styrene using hydrogen peroxide as an initiator and a soap as an emulsifying agent. These systems appear to conform most clearly to an ideal model system. There have been many other investigations with respect to the characterization of polymer latexes [6-8]. Stone and Watillon [9] found that the type of emulsifier used in the emulsion polymerization influences the stability of the dispersion, and the sensitivity to electrolytes, i.e. the critical coagulation concentration (ccc). It also influences the viscosity, the surface conductivity and the electrophoretic mobility of the latex. Ottewill et al. [10, 11] observed that there is no relation between the stability ratio curves and the particle size, but the ccc

depends on the type and the density of the surface charge and the presence of stabilizing materials. Matijevic et al. [12-14] investigated the effects of aluminium nitrate on the stability of different types of polymer latexes. It was found that the stability depends on the pH of the medium. Under certain pH conditions, the electrolyte reacts with water to form hydrolysed species, which are strongly adsorbed onto the negatively charged particles.

### *Materials and Methods*

The polymer latex dispersion was Litex BL 112, a product of Hüls AG, with a solid content of 50 %.

The latex dispersion was purified from the emulsifier and electrolyte by passing it through both cationic and anionic exchange resins. The cationic column was purified just before use by flowing  $2 \text{ mol dm}^{-3}$  hydrochloric acid through it, while  $1 \text{ mol dm}^{-3}$  sodium hydroxide was passed through the anionic one; the columns were then washed with distilled water till no acid or base reaction was observed. After this pretreatment of the columns, a 1 % polymer latex dispersion was passed through each column at a rate of  $150 \text{ cm}^3/\text{minute}$ .

The pH and conductivity titrations of the purified 1 % polymer latex dispersions were carried out with a Radelkis (Hungary) OP-204/1 pH-meter and an OK-102/1 conductometer, with  $0.0525 \text{ mol dm}^{-3}$  potassium hydroxide. The contents of the titration vessel were stirred with a magnetic stirrer.

Coagulation rates were determined by measuring the rate of change of the turbidity of the polymer latex with a

Spekol 10 (GDR) spectrophotometer at 456 nm. The output was recorded on a Radelkis (Hungary) OH-814/1 recorder.

The average particle diameter was measured with a MOM. 3180 Ultracentrifuge (Hungary) the sedimentation coefficient being determined by a method given in [15].

All chemicals used were of AR grade. Aluminium chloride was a product of Reachim, USSR. Potassium hydroxide and calcium chloride were from Reanal, Hungary. Lanthanum chloride was a Merck product.

## *Results and Discussion*

### *1. Surface characterization*

#### *1.1. Conductometric and potentiometric titrations*

The conductometric and potentiometric titrations of the purified polymer latex were performed to determine its surface charge density and intrinsic dissociation constant.

The results of the titrations are shown in Fig. 1. It can be seen from the conductivity curve that there are two break-points. This means that the particles of polymer latex bear two types of acidic groups. This is more evident from the conductivity measurements than from the potentiometric ones, where the end-point of the titration can not be determined with high accuracy.

The values of the equivalency points can be determined by extrapolation of the linear parts of the conductometric curve. The first point was found at 8.6 mmol/g solid, which is equivalent to the strong acidic groups on the surface of the polymer latex particles. The second one, at 124 mmol/g



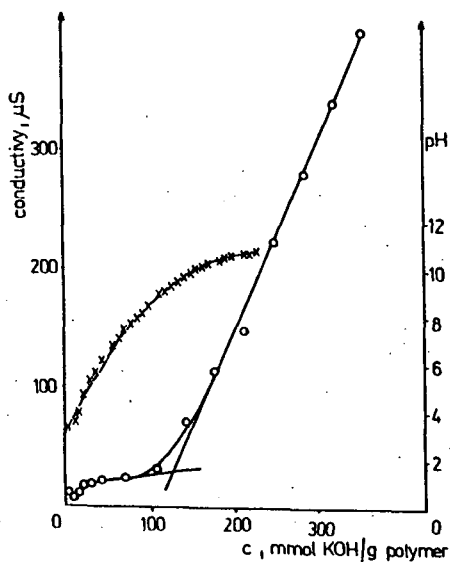


Figure 1: Conductometric and potentiometric titration of a polymer latex with KOH  
 (x) potentiometric curve  
 (o) conductometric curve

solid, corresponds to the total amount of all acidic groups on the surface of the polymer spheres.

The average size of the polymer spheres was calculated from the sedimentation coefficient of the particles of the latex. The average diameter was found to be 85 nm.

From the amount of acidic groups, the density of  $1.054 \text{ g/cm}^3$  for the polymer particles, the average particle diameter of 85 nm, and the supposition that the particles are spherical in form, the surface charge density was calculated to be  $0.15 \text{ } \mu\text{C/cm}^2$  for the strong acidic sites and  $3.6 \text{ } \mu\text{C/cm}^2$  for the total amount of acidic surface sites.

### 1.2. Intrinsic dissociation constant

The dissociation of acidic surface groups in a polymer latex may be characterized by determination of the intrinsic acidity constant,  $pK_{int}$ , as follows.

The degree of dissociation,  $\alpha$ , is the ratio between the amount of partially dissociated charges on the surface of polymer particles and their total amount. It can be calculated from the conductivity curve data. The apparent acidity constant is calculated from the titration data via the following equation [16]:

$$pK_a = pH_{solution} - \log \frac{\alpha}{1-\alpha}$$

$pH_{solution} - \log(\alpha/(1-\alpha))$  is plotted as a function of  $\alpha$ , and extrapolation of the straight part of the curve to  $\alpha = 0$  (Fig. 2) gives the intrinsic acidity constant,  $pK_{int}$ . This was determined to be 4.1. This value relates to the dissociation of weakly acidic groups on the surface. In this case, the determination of the intrinsic dissociation constant of the strongly acidic groups is not possible by this method, because their amount ( $8.6 \text{ mmol g}^{-1}$ ) is much smaller than that ( $115.4 \text{ mmol g}^{-1}$ ) of weakly acidic groups. Therefore some of the titration data relating to the first dissociation step can not be evaluated.

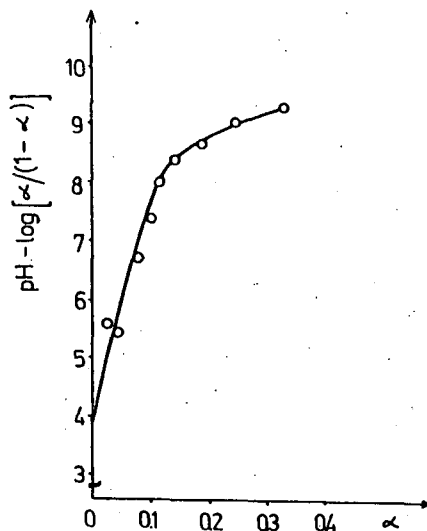


Figure 2: Relation between  $\text{pH} - \log(\alpha/(1-\alpha))$  and  $\alpha$

## 2. Stability of polymer latex dispersion

Measurements of the coagulation kinetics of the polymer latex dispersion were carried out to obtain information about its stability.

The number of particles  $N_t$  present in the dispersion at time  $t$  after the addition of electrolyte is given by the Smoluchowski equation [17]:

$$N_t = N_0 / (1 + kN_0 t)$$

where  $N_0$  is the number of particles in the initial dispersion, and  $k$  is the rate constant of coagulation, which can be put equal to  $k_0/W$ , where  $W$  is the stability ratio and  $k_0$

is the rate constant of rapid coagulation. The values of  $k_0$  and  $k$  can be determined experimentally in the rapid and the slow region of coagulation, respectively.

Measurements of the coagulation kinetics were carried out within 1 minute after electrolyte addition, by determination of the turbidity of the diluted dispersion. The slope of the turbidity vs time function could be taken as proportional to the initial rate of coagulation.

The change in turbidity is

$$\frac{d\tau}{dt} = v \cdot \text{constant}$$

where  $v$  is the rate of coagulation and the constant depends on the optical parameters of the measurements. If the initial concentrations are the same,

$$W_{\text{expt}} = \frac{v_{\text{fast}}}{v_{\text{slow}}}$$

Thus,

$$W_{\text{expt}} = \frac{v_{\text{fast}} \cdot \text{constant}}{v_{\text{slow}} \cdot \text{constant}} = \frac{d\tau/dt_{\text{fast}}}{d\tau/dt_{\text{slow}}}$$

The variation in turbidity of the dispersion for different amounts of aluminium chloride is presented as an example in Fig. 3. It can be seen that the slope of the curves increases up to a certain value with increasing amount of electrolyte.

The stability of the polymer latex is characterized by plotting  $\log W_{\text{expt}}$  against  $\log$  molar concentration of the electrolyte. The ccc can be calculated by extrapolating the  $\log W_{\text{expt}}$  values to  $\log W_{\text{expt}} = 0$ . The intercept on the  $\log c$  axis gives the ccc.

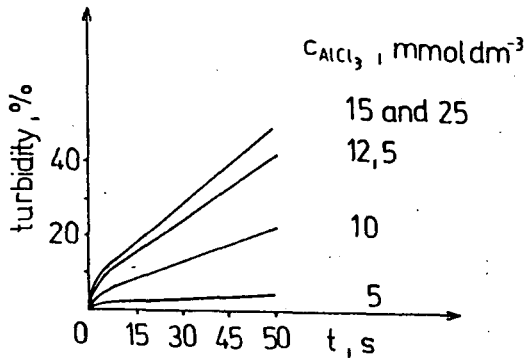


Figure 3: Effect of  $\text{AlCl}_3$  amounts on turbidity of polymer latex as a function of time

### 2.1. Effect of electrolyte concentration

The effects of the electrolyte concentration on the stability of the polymer latex dispersion were studied by using calcium chloride as a divalent electrolyte and aluminum chloride and lanthanum chloride as trivalent electrolytes. The variation of  $\log W_{\text{expt}}$  with  $\log c$  is shown in Fig. 4.

From the Figure, the values of  $\text{ccc}$  are 34, 15.8 and 2  $\text{mmol dm}^{-3}$  for  $\text{CaCl}_2$ ,  $\text{AlCl}_3$  and  $\text{LaCl}_3$ , respectively. The  $\text{ccc}$  of  $\text{LaCl}_3$  is in good agreement with that obtained by others [12, 18], but it differs from that of  $\text{AlCl}_3$ . This may be due to the interaction of  $\text{AlCl}_3$  with water. Matijevic et al. [12-14] found that the  $\text{Al}^{3+}$  ion exists in different hydrolysis forms at  $\text{pH} < 3.3$ . As the  $\text{pH}$  increases, reaction occurs with water to form a sequence of hydrolysed species.

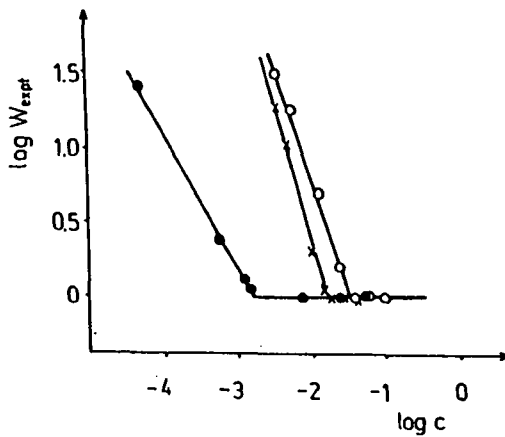


Figure 4: Stability of polymer latex dispersion as a function of electrolyte concentration in mol dm<sup>-3</sup>.

- (o) calcium chloride
- (x) aluminum chloride
- (●) lanthanum chloride

The pH of the dispersion was measured after electrolyte addition. It was found that the AlCl<sub>3</sub> electrolyte decreases the pH of the dispersion to a large extent, while LaCl<sub>3</sub> and CaCl<sub>2</sub> have smaller effects on it. The ratio of the ccc values for CaCl<sub>2</sub> and AlCl<sub>3</sub> was 2.1, whereas that for CaCl<sub>2</sub> and LaCl<sub>3</sub> was 17, in approximate agreement with the theoretical value of 11.4 to be expected from the valency rule.

## References

- [1] *Myseles, K.J.*: Introduction to Colloid Chemistry, 4th Printing, Interscience Inc., N.J., (1967).
- [2] *Hogg, R., T.W. Healy and D.W. Fuerstenau*: Trans. Faraday Soc. 62, 1638 (1966).
- [3] *Ottewill, R.H. and R.F. Woodbridge*: J. Colloid Sci. 18, 581 (1961).
- [4] *Ottewill, R.H. and R.F. Woodbridge*: J. Colloid Sci. 19, 606 (1964).
- [5] *Shaw, J.N. and R.H. Ottewill*: Nature, 208, 281 (1965).
- [6] *van den Hul, H.J. and J.W. Vanderhoff*: J. Colloid Interface Sci. 28, 336 (1968).
- [7] *McCann, G.D., E.B.B. Bradford, H.J. van der Hull, and J.W. Vanderhoff*: in Polymer Colloids, R.M. Fitch (ed.), Plenum Press, New York, p. 29 (1971).
- [8] *Ottewill, R.H. and J.N. Shaw*: Kolloid Z.Z. Polym. 215, 161 (1967).
- [9] *Stone-Masui, J. and A. Watillon*: J. Colloid Interface Sci. 28, 187 (1968).
- [10] *Ottewill, R.H. and J.N. Shaw*: Discuss. Faraday Soc. 42, 154 (1966).
- [11] *Buscall, R. and R.H. Ottewill*: in Polymer Colloids, Buscall, R., T. Corner and J.F. Stegeman (eds), Ch. 5., Elsevier, London, p. 141 (1985).
- [12] *Force, C.G. and E. Matijevic*: Kolloid Z.Z. Polym. 225, 33 (1968).
- [13] *Force, C.G. and E. Matijevic*: Kolloid Z.Z. Polym. 224, 51 (1968).
- [14] *Matijevic, E.*: J. Colloid Interface Sci. 58, 374 (1977).
- [15] *McCormick, H.W.*: J. Colloid Sci. 19, 173 (1964).
- [16] *Homola, A. and R.O. James*: J. Colloid Interface Sci. 59, 123 (1977).
- [17] *Smoluchowski, M.*: Z. Phys. Chem. 92, 129 (1917).
- [18] *Ottewill, R.H. and T. Walker*: Kolloid Z.Z. Polym. 227, 108 (1968).

## ЭФФЕКТ КОНЦЕНТРАЦИИ ЭЛЕКТРОЛИТА НА СТАБИЛЬНОСТЬ ПОЛИМЕРНОГО ЛАТЕКСА

А. А. Абд Эл Хахим, Э. Томбац и Ф. Санто

С применением потенциометрической и кондуктометрической титрования характеризуется поверхностный заряд полимерного латекса (фирмы Hüls AG) Litex VL 112. Было показано наличие кислотных групп двух типов: небольшое количество сильнокислотных и большее слабокислотных групп, образующих поверхностную плотность заряда  $3.6 \text{ мк/см}^2$ . Постоянная кислотной диссоциации была найдена равной 4.2. Определены критические концентрации коагуляции для  $\text{CaCl}_2$ ,  $\text{AlCl}_3$  и  $\text{LaCl}_3$ , которые составляли 34, 15.8 и 2 ммоль/дм<sup>3</sup> соответственно.



## DRUG-CONTAINING MULTIPLE-PHASE EMULSIONS

By

J. BALÁZS<sup>1</sup>, I. ERŐS<sup>2</sup>, M. TACSI<sup>2</sup> and I. PÉTER<sup>1</sup>

<sup>1</sup> Department of Colloid Chemistry, József Attila University  
Szeged, Hungary

<sup>2</sup> Department of Pharmaceutical Technology, Albert  
Szent-Györgyi Medical University, Szeged, Hungary

(Received 15 June 1988)

We studied the effectiveness of the formation of w/o/w emulsions as a function of composition and mixing time. We found that concentration of emulsifier 1, the concentration and HLB of emulsifier 2, the viscosity of the oil phase and the external water phase as well as the mixing time in step two of making the emulsion characteristically influence the effectiveness of emulsification and the stability of the emulsions.

### *Introduction*

The "complex" emulsions (multiple phase emulsions, dop-pelte Emulsionssysteme) are disperse systems in which the disperse phase contains droplets of the external (coherent) phase. Two types are known: "water-in-oil-in-water" (w/o/w) and "oil-in-water-in oil" (o/w/o) [1].

As concerns the structure of w/o/w emulsions, water droplets in an oil coating are present in a coherent water phase ( $w_2$  phase, "external" water phase) [2,3] (Fig. 1).

The prospective uses of these systems justify investigations of their formation, properties and stability. Hungarian research in this field began only recently [4,5].

So far, the chemical industry, the food industry and the drug industry apply complex emulsions [1]. Their use as drug delivery systems seems especially important and promising.

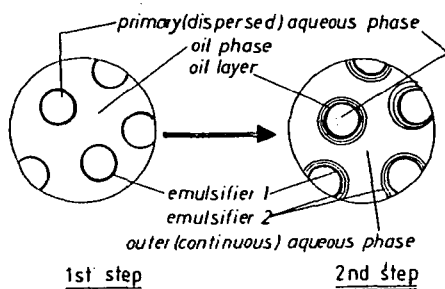


Figure 1.: Two-step procedure for emulsification and structure of w/o/w emulsions [3].

Their application in pharmaceuticals is based on their following favourable properties [6-8]:

- protection of an agent dissolved in an internal water (or oil) phase is ensured,
- a prolonged effect can be achieved,
- in cases of overdosing, they have a detoxicating effect.

w/o/w and o/w/o emulsions have so far been used with more or less success in the formulation of vaccines, analgetics and antiphlogistics, hormone preparations, antitumour

agents, antibiotics and morphine antagonists [6-12].

For the production of stable w/o/w emulsions, the following are necessary:

- a non-ionic emulsifier with a low HLB value in a relatively high concentration (in order to form a w/o emulsion),
- an emulsifier with a high HLB value in a relatively low concentration (ensuring dispersion of the w/o emulsion in the coherent water phase),
- a suitable volume of the w/o emulsion within the complex emulsion [2, 3, 12].

The aim of our investigations was to develop a stable w/o/w emulsion. Our primary task was to elucidate the relationship between the composition, and especially the concentrations of the two emulsifiers, and the result of emulsification. We set out to improve the stability (at the optimum composition) by increasing the viscosity of the external water phase and by thickening the oil phase. A further aim was to learn whether a stable w/o/w emulsion is suitable as a drug delivery system. At what rate and in what quantities is the active substance liberated from the complex emulsions?

The present paper reports on studies concerning the effectiveness of production of w/o/w emulsions.

#### *Materials and methods*

w/o/w emulsions were made from liquid petrolatum (Paraffinum liquidum, satisfying Ph.Hg.VI), Span 80, Span 20 and Tween 80 (Atlas GmbH, FRG). The viscosity of the external water phase was improved with hydroxyethyl-cellulose (Cellosize QP, Union

Carbide, USA). The oil phase was thickened with ceresine. Emulsions were prepared in a two-step procedure [2,3]. In the first step, Span 80 (lipophilic emulsifier) was dissolved in liquid paraffin, after which water was emulsified in it by mechanical stirring at an even rate. The internal water phase of the model emulsions was a  $10^{-1} \text{ mol dm}^{-3}$  potassium chloride solution; the drug-containing emulsions contained 1 mass per cent of ephedrinium chloride solution. In the second step, the w/o emulsion obtained in this way was emulsified in an aqueous solution of Tween 80 (hydrophilic emulsifier) or a Tween 80-Span 20 mixture.

*Investigation of "efficiency" of formation of emulsions*

The efficiency of formation of the complex emulsion was determined as the proportion of chloride ions added to the internal water phase which penetrated into the external water phase:

$$\text{efficiency (\%)} = \frac{c_{\text{KCl}} - \text{measured } c_{\text{KCl}}}{c_{\text{KCl}}} 100 \quad (1)$$

Chloride ion concentration was measured with a Radelkis OP-CI-0711 P membrane electrode and a Radelkis OR-205/1 precision pH and voltage-meter immediately after emulsification and after different periods of waiting.

*Investigation of drug release*

The liberation of ephedrinium chloride dissolved in the internal water phase was studied by the membrane dialysis method (leading to equilibrium). A synthetic membrane was attached to one end of the dialysing tube, and a constant volume of emulsion was measured on it. The tube was placed in a flask containing 20.0 ml distilled water at body temperature. The membrane just touched the surface of the water. This apparatus was placed in a thermostat at 305 K. The amount of ephedrinium chloride that passed through the membrane was measured with a Spektromom 195 spectrophotometer at 290 nm. Examination of the liberation of the agent was also found to be suitable for numerical characterization of the efficiency of emulsification. In agreement with the literature, a linear correlation was obtained between the amount of ephedrinium chloride measured in the dialysis liquid ( $Q$ ) and the square root of the time of dialysis ( $t$ ) [14]:

$$Q = a \sqrt{t}. \quad (2)$$

$a$  is the rate of liberation of the agent. We determined the rates of liberation of the drug from the w/o emulsion and from a w/o/w emulsion that contained ephedrinium chloride in the external water phase. If the two steps of emulsification were perfect, then the rate of dialysis would be rate of liberation of drug from the w/o emulsion. If no w/o/w emulsion was formed in step 2, but all of the agent passed into the external water phase, then the rate of drug release would be that of a w/o/w emulsion in which the agent was already dissolved in the external water. Therefore, if we consider the first 100 and the latter 0 % emulsifications, with

a known rate constant of dialysis, we can determine the efficiency of the emulsion formation by means of a nomogram (calibration line, Fig. 2):

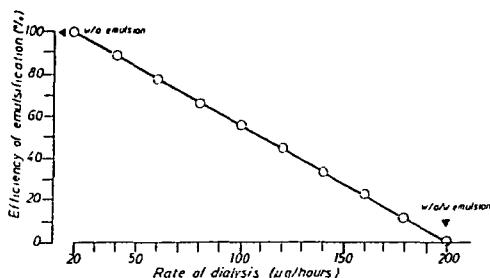


Figure 2.: Efficiency of emulsification determined via rate of dialysis

### *Rheological examinations*

Rheological measurement (leading to flow and viscosity curves) were made with a Rheotest-2 and a Höppler rheoviscometer at 298 K.

### *Results and discussion*

#### *1. Effect of composition on effectiveness of emulsification*

The effectiveness of formation of w/o/w emulsions is mainly influenced by the amount of lipophilic emulsifier [1-3]. In the studies on the production of stable emulsions,

the amount of lipophilic emulsifier was varied at constant amount of hydrophilic emulsifier and volume ratio. It can be seen from Fig. 3 that the effectiveness of emulsification increased with the concentration of emulsifier 1, but even in the presence of 20 % lipophilic emulsifier only 70 % complex emulsion was formed. Figure 3 shows the correlation between the volume ratio and effectiveness. The effectiveness of emulsification increased with increase of the volume of the o/w emulsion.

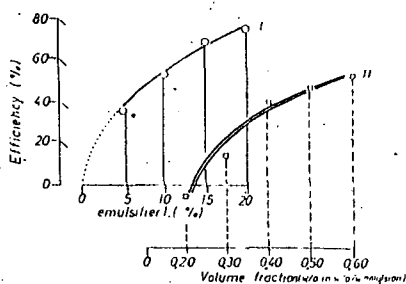


Figure 3.: Effects of concentration of lipophilic emulsifier (I) and volume fraction (II) on formation of w/o/w emulsions

In the next phase, the concentration of the second emulsifier (Tween 80) was also changed. Figure 4 shows an interesting phenomenon. In the presence of 0.1 % hydrophilic emulsifier, emulsification was complete, but then not a liquid emulsion, but a cream-like substance with a specific structure was formed. An increase of the amount of the hydrophilic emulsifier sharply reduced the effectiveness of emulsification until a minimum was reached. Further increase of the concentration led to a maximum in the graph of the function. On increase of the concentration of the lipophilic

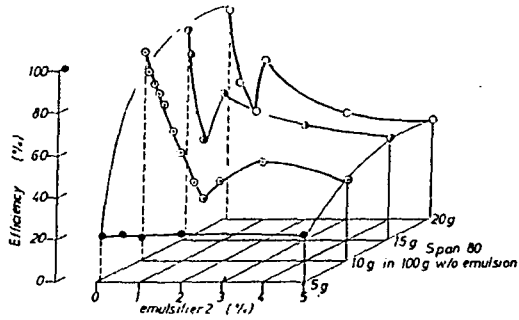


Figure 4.: Effect of emulsifier 2 concentration on formation of w/o/w emulsions

emulsifier, the maximum is situated at lower and lower concentrations of emulsifier 2.

The HLB value of the hydrophilic emulsifier also influences the effectiveness of emulsification: the correlation between HLB and effectiveness exhibited a maximum. With increase of the concentration of emulsifier 1, the optimum HLB shifted towards higher values.

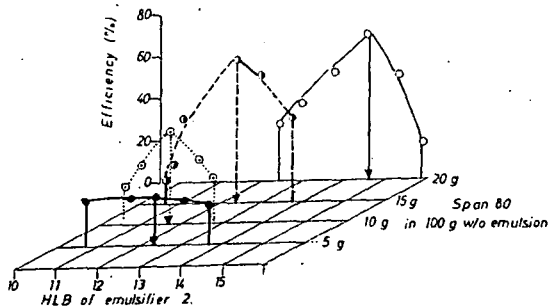


Figure 5.: Effect of HLB on formation of w/o/w emulsions



2. Drug release from w/o/w emulsions. Evaluation of effectiveness of emulsification via rate of dialysis

The emulsion deemed most suitable on the basis of its effectiveness was used to prepare a drug-containing emulsion. One mass per cent of ephedrinium chloride was dissolved in either the internal or the external water phase. The process of liberation of the agent was studied (Fig. 6).

In this series of experiments the stability of the emulsions and the effectiveness of emulsification were closely connected: the rate constant of the 8-hour dialysis was determined and used to calculate the effectiveness of emulsification via Fig. 2. The effectiveness determined in this was characterized the stability. If the rate of dialysis was low (i.e. not higher than the rate of the w/o emulsion), then emulsification was successful and the emulsion remained stable for 8 hours.

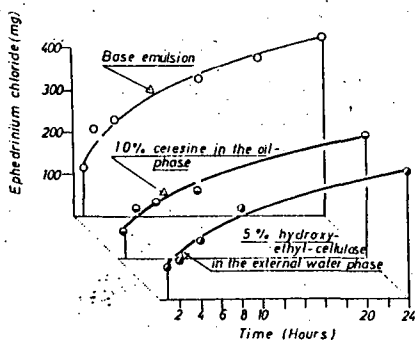


Figure 6.: Drug release from w/o/w emulsions

The effectiveness of emulsification was found to be increased considerably by an increase of the viscosity of the oil phase (addition of ceresine). Increase of the viscosity of the continuous water phase with hydroxyethyl-cellulose had less effect on the stability. The duration of emulsification was of vital importance: mixing for a longer time than optimum or just necessary destroyed the w/o/w emulsion (Table I).

Investigation of the relationship between the stability values calculated on the basis of dialysis and the results of ion-selective membrane electrode examinations is continuing.

*Table I*  
*Effectiveness of formation of w/o/w emulsions*

	<i>COMPOSITION</i>	<i>EFFICIENCY (%)</i>
<i>Base emulsion</i>	<i>10 g Span 80 in 100 g w/o emulsion</i>	
	<i>1 g Tween 80 in 100 g w/o/w emulsion</i>	<i>67,9</i>
	<i>0,4 volume fraction (w/o in w/o/w)</i>	
<i>Increase of viscosity of oil phase</i>	<i>0 % ceresine</i>	<i>67,9</i>
	<i>5 % ceresine</i>	<i>78,0</i>
	<i>10 % ceresine</i>	<i>79,9</i>
<i>Increase of viscosity of continuous w phase</i>	<i>3 % HEC</i>	<i>75,9</i>
	<i>4 % HEC</i>	<i>74,3</i>
	<i>5 % HEC</i>	<i>75,4</i>
<i>Time of 2nd step (mixing time)</i>	<i>1 minute</i>	<i>80,9</i>
	<i>3 minutes</i>	<i>63,3</i>
	<i>5 minutes</i>	<i>40,4</i>

### 3. Rheological investigation of w/o/w emulsions

The development of w/o/w emulsions from w/o emulsions involves important rheological changes. From the structurally viscous w/o emulsion with high viscosity, ideally viscous systems with much lower viscosity are formed (Fig. 7).

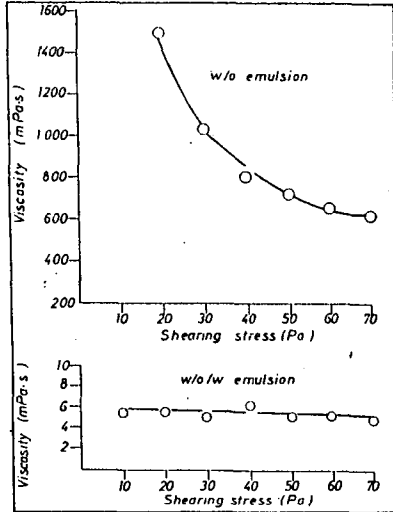


Figure 7.: Viscosity curves of w/o and w/o/w emulsions

Dissolution of the polymer in the external water phase increases the viscosity of w/o/w emulsions (Fig. 8).

Comparison of the viscosity curves of the emulsions made with different mixing times (Fig. 9) proved our assumption that, during a long mixing time, w/o/w emulsions undergo transformation into simple o/w emulsions. The viscosity

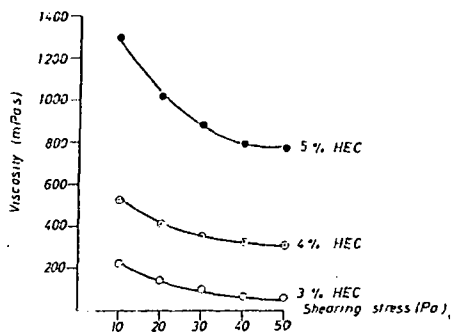


Figure 8.: Effect of hydroxyethyl-cellulose (HEC) content on viscosity of w/o/w emulsions

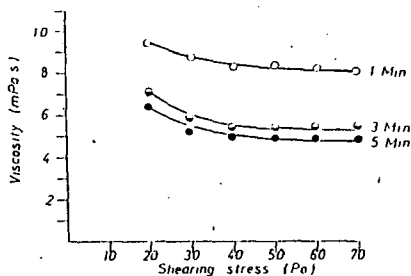


Figure 9.: Effect of mixing time (2nd step) on viscosity of w/o/w emulsions

of a w/o/w emulsion made by mixing for 5 minutes is about half that of an emulsion made by mixing for 1 minute.

## References

- [1] *Attwood, D. and A.T. Florence: Surfactant Systems. Their Chemistry, Pharmacy and Biology.* Chapman and Hall, London, New-York, 1983. pp. 509-519.
- [2] *Matsumoto, S., Y. Koh and A. Michiura: J. Dispers. Sci. Technol.* 6, 507 (1985).
- [3] *Matsumoto, S., Y. Kita and D. Yonezawa: I. Coll. Interface Sci.* 57, 353 (1976).
- [4] *Baldzs, J., I. Erős, M. Tacsi and I. Péter: 1st International Congress on Cosmetics and Household Chemicals Abstracts 108, Budapest, 1987.*
- [5] *Erős, I., J. Baldzs and Sz. Mueztafa: ibid 104*
- [6] *Brodin, A.F., D.R. Kavaliunas and S.G. Frank: Acta Pharm. Suec.* 15, 1 (1978).
- [7] *Brodin, A.F. and S.G. Frank: ibid 15, 111 (1978).*
- [8] *Mcrimoto, Y., K. Sugibajashi and Y. Yamaguchi: Chem. Pharm. Bull.* 27, 3188 (1979).
- [9] *Schichiri, M., Y. Shimuzu: Diabetologica* 10, 317 (1974).
- [10] *Muranishi, S., Y. Takahashi, M. Hashida and H. Sezaki: J. pharm. Dyn.* 2, 383 (1979).
- [11] *Tomita, M., Y. Abe and T. Kondo: J. pharm. Sci.* 71, 332 (1982).
- [12] *Abd-Elbary, A., S.A. Noyr and F.F. Mansour: Pharm. Ind.* 46, 964 (1984).
- [13] *Matsumoto, M.: Formation and Stability of Water-in-Oil-in-Water Emulsions. In Macro and Microemulsions: Theory and Applications (Ed.: D.O. Shah). American Chemical Society, 1985. pp. 415-436.*
- [14] *Thoma, K.: Dermatika. Werbe- und Vertriebsgesellschaft Deutscher Apotheker m.b.H. München, 1983.*

## ДРОГ-СОДЕРЖАЩИЕ МНОГОКРАТНЫЕ ЭМУЛЬСИИ

Я. Балаж, И. Эреш, М. Тачи и И. Петер

Изучена эффективность образования эмульсий в/м/в в зависимости от состава и времени перемешивания. Показано, что на эффективность образования многократных эмульсий и на их стабильность оказывают определяющее влияние концентрация эмульгатора 1, концентрация и ГЛБ эмульгатора 2, вязкость масляной и водной фаз, а также время перемешивания во второй ступени приготовления эмульсии.

## INDEX

L. MICHAÏLOVITS, M.I. TÖRÖK and I. HEVESI: On the Error of the Absorption Coefficients of Weakly Absorbing Thin Layers, Determined from Transmittance Measurements . . . . .	3
J. CSÁSZÁR: Comparison of the UV Spectra of Aromatic Schiff Bases and Their Reduction Products; Possibility of Assignment of $\pi^* + n$ Transition of Azomethine Group . . . . .	17
J. CSÁSZÁR: Study of the Spectral Behaviour of molecular Complexes of Picric Acid and Hexanitrobiphenylamine with Schiff Bases Formed from Salicylaldehyde and Alkylamines, Polymethylenediamines, Sulphonamides and Aminopyridines . . . . .	29
P. NAGY and R. HERZFELD: Solvent Effect in the Formation of Schiff Bases . . . . .	51
H. SCHOLL and P. KRZYCZMONIK: Electrode Processes of Derivatives of 2,2,4,4-Tetramethylpentane on Stationary Solid Electrodes I. Cyclic Voltammetry of 3-Hydrazones of 2,2,4,4-Tetramethylpentane . . . . .	65
H. SCHOLL and P. KRZYCZMONIK: Electrode Processes of Derivatives of 2,2,4,4-Tetramethylpentane on Stationary Solid Electrodes II. Voltammetry of 3,3'-Dibromo-2,2,4,4-Tetramethyl-Pentane in DMF . . . . .	83
A.A. ABD EL HAKIM, E. TOMBÁ CZ and F. SZÁNTÓ: Stability of $TiO_2$ Dispersions at Different pH Values and in Presence of $AlCl_3$ Electrolyte . . . . .	99
A.A. ABD EL HAKIM, E. TOMBÁ CZ and F. SZÁNTÓ: Effect of Electrolyte Concentration on Stability of Polymer Latex . . . . .	109
J. BALÁZS, I. ERŐS, M. TACSI and I. Péter: Drug-Containing Multiplex-Phase Emulsions . . . . .	121



Fk: Dr. Gécseg Ferenc

Készült a JATE Sokszorosító Uzemében, Szeged

Engedélyszám: 143/89. Méret: A/5

Példényszám: 425

Fv: Lengyel Gábor